РЕЗЮМЕТА

на научноизследователските трудове
на ас. д-р инж. Татяна Миткова Мечкарова,
в катедра „Материалознание и технология на материалите“, при Технически университет – Варна
за участие в конкурс публикуван в Държавен вестник, брой № 2, 05.01.2024г.
за заемане на академична длъжност „доцент“,
обявен в професионално направление „5.1. Машинно инженерство“,
по дисциплината „Технология на материалите“

Summaries according to indicator B.4 - that are referenced and indexed in world- databases.

B.4.1. Yordanov K., Mechkarova T., Stoyanova A., Zlateva P., Determination of the Temperature of Cathode Unit of Indirect Plasma Burner Through a Computer Simulation Model, Proceedings of the Second International Scientific Conference “Intelligent information technologies for industry” 2017, Vol. 2, ISSN: 2194-5357, pp 403-409, https://doi.org/10.1007/978-3-319-68324-9_44

Abstract: The article is developed computer simulation analysis of the spread heat flows in indirect torch for gas nitriding, using the software Autodesk CFD. Different methods of using a stream of ionized plasma as a sourse of energy are applied early 50 s of last century, but only in recent years, they are widely used in chemical heat metal processing. One of new highly productive methods for hardening a titanium surface is the plasma nitriding with indirect plasma torch.

Fig. 1

Conclusion:

Fig.1 shows the result of the computer thermal analysis for the distribution of the temperature fields in the cathode and anode assemblies using the Autodesk Simulation CFD software product. On the left, the program displays in graphic form with numbers and colors the reported temperatures that are registered in the different volumes of the 3D model on the right. Fig. 1 shows the result for the 10th s when maximum temperatures of 2170°C to 2200°C were recorded.

The results of the computer simulation model are compared to those of real experimetal testing of the plasma burner, with the divergence being c permissible limits.

B.4.2. Stoyanova, A., Mechkarova, T., Konsulovabakalova, M., Yordanov, K., Argirov, Y., Investigation of strained and deformed state of low carbon plates after welding, UPB Scientific Bulletin, Series D: Mechanical Engineering, 2020, 82(3), ISSN 1454-2358, pp. 263-274, https:// www.scientificbulletin.upb.ro/rev_docs_arhiva/fullbd3_727198.pdf

The work is shown manual metal arc welding of steel with covered electrode.

The study of the heat exchange processes and occurrence of the deformations andtensions during welding of steel plates is presented. For this purpose, a simulation analysis of the object was developed. Results for strain and deformation distributions at each point in the volume of the studied model were obtained by thermal and static analysis. Determination of stresses and deformations after welding under the conditions of non-stationary heat exchange and elastic-plastic displacement of the metal led to the necessity to use approximate methods by applying modern programming means.

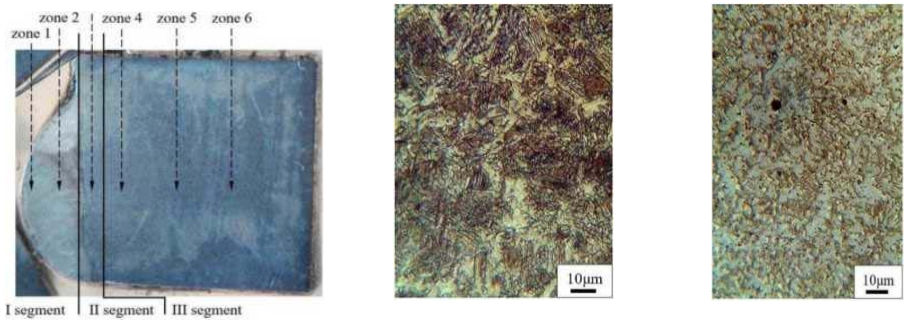

Fig.2. Macro and microstructures of the welded specimens

A computer simulation analysis of three-dimensional has also been developed the modeled specimens. The temperature distribution results and deformations are shown in Fig.3.

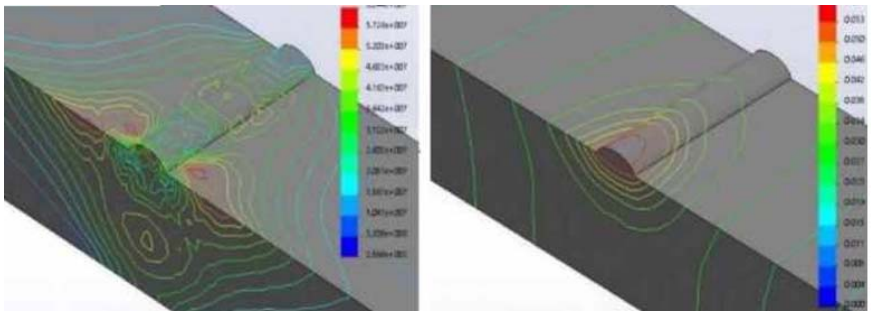

Fig.3. Computer simulation analysis termal stress and deformation

Conclusion: The results of the simulation analysis are fully consistent with the theoretical formulations regarding the occurrence and distribution of thermal stresses in hardfacing welding of the model under study..

B.4.3. Stoyanova, A., Mechkarova, T., Konsulovabakalova, M., Yordanov, K., Argirov, Y., Computer simulation thermal analysis of low carbon plates welded with electrode abradur64, UPB Scientific Bulletin, Series D: Mechanical Engineering, 2020, 82(4), ISSN 1454-2358, pp. 179-190, https://www.scientificbulletin.upb.ro/rev_docs_arhiva/ fulla6f_279381.pdf

Purpose: In this work, a computer simulation model has been used for heat transfer process study in steel plates that were Manual Metal Arc Welded. The heat transfer process evolution was simulate using SolidWorks Thermal Analysis. The base material used for study was steel DD11, on which a hard deposit using ABRADUR 64 welding electrodes has been performed. The temperature distribution in the different areas of Heat Affected Zone has been determined, according the welding regime parameters. The simulation model of heat transfer during welding has demonstrate that at the surface level, the steel plates do not reach a high values of temperature which can promote some microstructural changes in the heat affected zone.

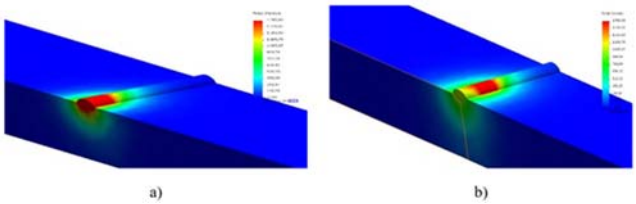

Fig.4. Computer simulation analysis for temperature distribution when welding DD11 steel with ABRADUR64 electrode

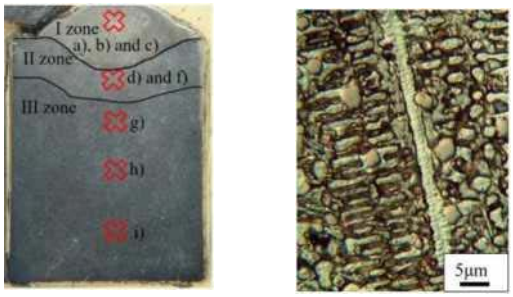

Fig.5. Metallographic analysis of macro and microstructure.

Conclusion: On the basis of the created computer model, it was found that in MMA hardfacing welding of the samples, the area of thermal impact does not reach the critical temperature, which is a prerequisite to believe that there will be no structural changes in it leading to destruction. This is evidenced by the metallographic analysis.

B.4.4. Stoyanova A., Mechkarova T., Argirov Y, Konsulova-Bakalova M., Atanasov, N., Study of structure and physico-mechanical properties of welding joints on vessel tank of austenite steel SS316, IOP Conference Series: Materials Science and Engineering , Volume 843, Issue 1, 26 May 2020, Art. number No 012013, ISSN17578981, DOI: 10.1088/1757-899X/843/1/012013

Purpose: The article addresses some problems related to the occurrence of cracks and defects in welding joints on a horizontal steel vessel tank after machine gas metal arc welding (GMAW). Tests have been carried out on the structure and mechanical properties of the welding joints between the cylinder and elliptical bottoms made of austenite steel SS316. Proven methodologies of microstructural and X-ray analysis were used to investigate the changes in the structure (weld seam, heat affected zone and base metal). The mechanical characteristics are determined by measurements of macro- and micro-hardness by Vickers and of static tension

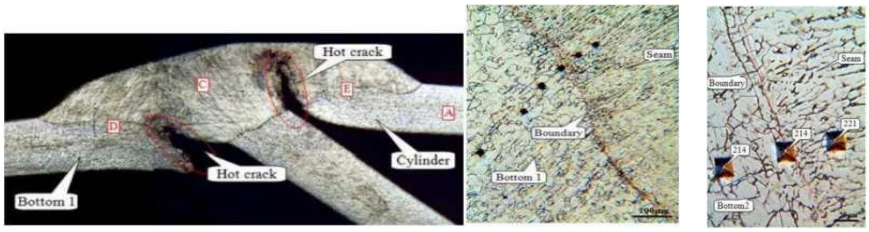

Fig. 6. Macro, microstructures and Vickers

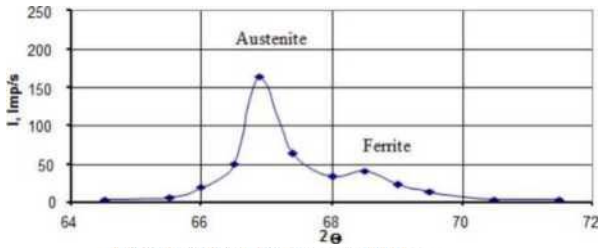

Fig. 7 X-ray phase analysis

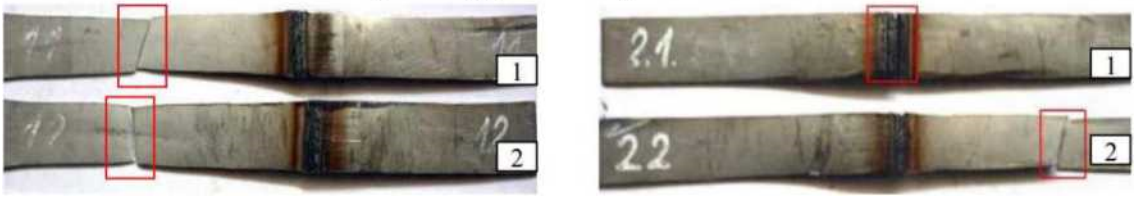

Fig. 8 Mechanical tensile

Conclusion: The profile of the seam in the tested section is well shaped but again displaced, this time in the direction of the cylinder, due to which part of the contact zone between Bottom 2 and the cylinder is not alloyed; the penetration into the material at Bottom 2 is weak, and into the cylinder it is incomplete. As a result, the root of the seam has a large open surface.

B.4.5. Argirov Y., Mechkarova, T., Stoyanova A., Atanasov, N., Konsulova-Bakalova, M., Study on structure and mechanical properties of 20X13 steel welding joints, IOP Conference Series: Materials Science and EngineeringVolume 843, Issue 1,26 May 2020, Art. number No 012012, ISSN17578981, DOI: 10.1088/1757-899X/843/1/012012

Purpose: The article deals with the problem related to the methods of control of the structure and mechanical properties of welding joints formed during the recovery of riveted joints on turbine blades made of 20X13 steel (AISI, 420J2). For the purposes of the study, the methodologies used are for microstructural analysis, micro- and macro-hardness of two types of samples: one without further heat treatment and the other with heat treatment after the process of welding.

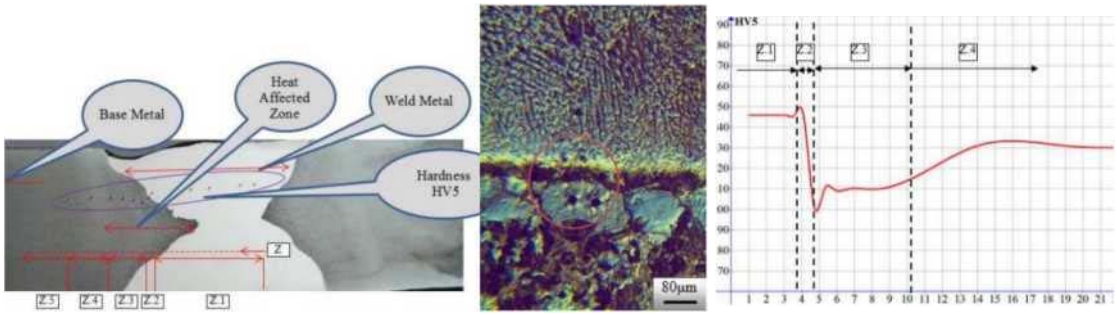

Fig. 9. Macro, microstructures and Vickers microhardness HV0.05

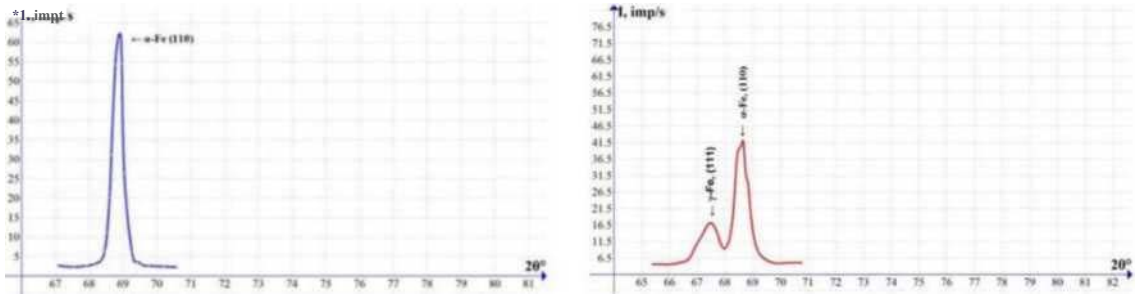

Fig. 10. X-ray phase analysis

Conclusion: From the conducted structural tests, the data was collected about the following zones and structures after welding: the alloying zone (the zone of partial melting of the base metal), the precrystallization zone (Ac1, 820oC-Ac3, 950oC), the heat affected zone including the two zones and the zone of the base metal in the investigated samples. It can be noted that in the heat affected zone there is no sudden increase in hardness, but a gradual increase towards the base material.

B.4.6. Spasova D., Argirov Y., Mechkarova T., Comparative Analysis of the Mechanical Properties of Polymer Matrix Composites Reinforced with Fiberglass Fabric, TEM Journal, 2021, Volume 10, Issue 4, pp. 1745 - 1750, ISSN22178309, DOI: 10.18421/TEM104-35

Objective: Analyzing the mechanical properties of six types of composite materials with a polymer matrix and reinforced with fiberglass fabric. Two types of resin were used for the matrix - polyester and vinylester. Both types of matrices are reinforced with three different fabrics of monoaxial, biaxial and triaxial fiberglass. The studied composites were obtained by mechanical pressing in the form of six-layer flat samples. Analysis consists of bending strength research and macrofractographic analysis.

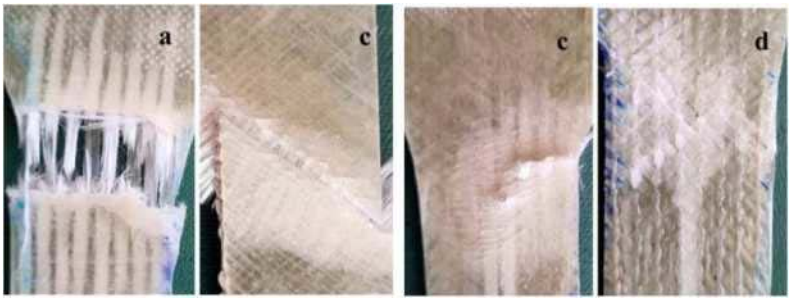

Fig. 11. Macrostructures of the test bodies after testing the strength of bending

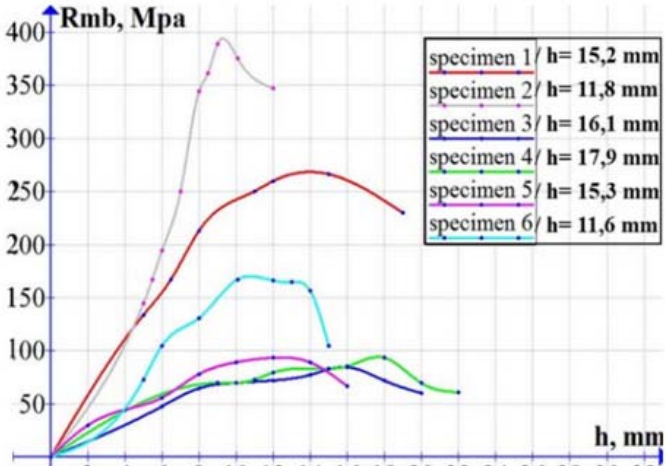

Fig. 12. Results of the flexural strength analysis

Conclusion: After the tests, the highest strength is showed monoaxial fiberglass followed by triaxial fiberglass, and the lowest characteristics of mechanical strength is given biaxial fiberglass, but it gives the largest vertical displacement, i.e has higher ductility.

B.4.7. Spasova D., Argirov Y., Mechkarova T., Comparative Analysis of the Mechanical Properties of Polymer Matrix Composites Reinforced with Fiberglass Fabric, TEM Journal, 2021, Volume 10, Issue 4, pp. 1745 - 1750, ISSN22178309, DOI: 10.18421/TEM104-35

Purpose: This paper is related to the production and investigation of the structure, the mechanical and physicochemical properties of two kinds of fibre reinforced polymer matrix composites in order to assess their suitability as materials used in equipment operating in marine environment. The one of the investigated composites has a polyester resin matrix and a reinforcement phase of six-layer fibreglass, and the other one has a vinylester resin matrix and a reinforcement phase which is a combination of three-layer fibreglass and three-layer biaxial fibreglass. A comparative analysis has been made of the relative weight, tensile strength and bending strength of the two types of composite materials.

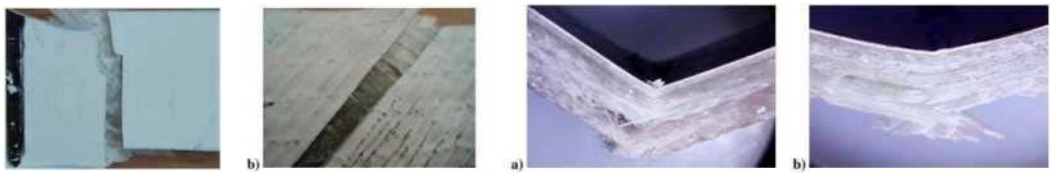

Fig. 13. Macrostructures after testing tensile and bending strength

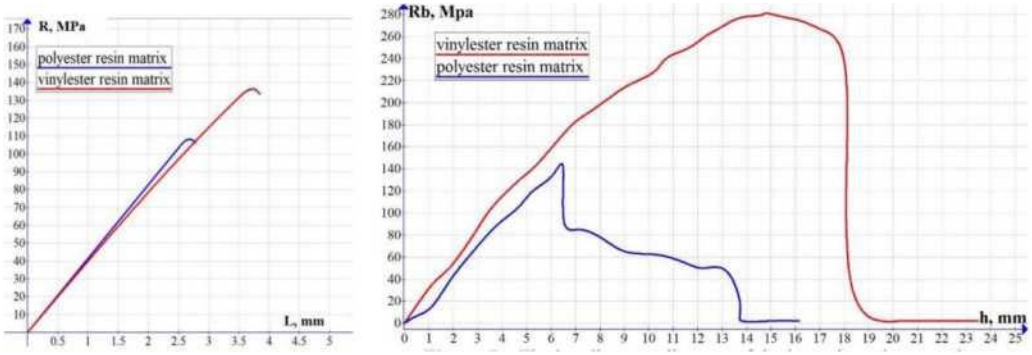

Fig. 14. Tensile and flexural strength analysis results

Conclusion: The density of both materials is approximately the same, lower than that of the traditional metallic materials used for manufacturing equipment operating in marine environment. BRVMCs have higher tensile strength and significantly higher bending strength compared to FRPMCs, which is mainly due to the fact that its reinforcement phase is composed not only of fiberglass but also of biaxial fabric. Both composite materials are suitable for the construction of equipment and facilities operating in marine environment, but BRVMCs would be the more suitable material as compared to FRPMCs.

B.4.8. Georgiev G., Argirov Y., Mechkarova T., Spasova D., Stoyanova A., Investigation of the occurrence and development of fatigue cracks after corrosion of welded samples of ferritic-austenitic steel, IOP Conference Series: Materials Science and Engineering, Volume 1037, Issue 1, 11 February 2021 Art. number No 012037, ISSN17578981, DOI: 10.1088/1757-899X/1037/1/012037

Objective: The article treats the occurrence and development of fatigue cracks in welded samples of ferritic - austenitic steel, which were previously subjected to corrosion. For the purposes of the study, two groups of sheet steel samples were prepared: the first group were reference parts, and the second group of samples were welded and then exposed to a corrosive environment.

Corrosion tests were performed by immersing the samples in an acidic solution of (HCl, HNO3 and NaCl). Both groups of samples were tested with specially developed vibrating equipment for high cycle fatigue (106 - 107 cycles). The durability of SAF 2507 steel is estimated by the number of cycles until a crack is obtained at a certain alternating load. The damaged surfaces were examined by microstructural analysis to trace the shape and development of the crack in the structure of ferro-austenitic steel SAF 2507 after its welding and corrosion.

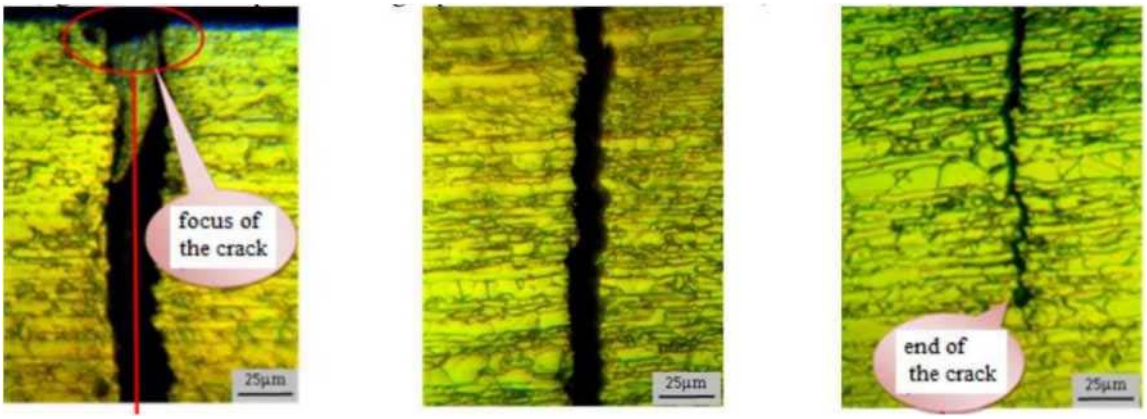

Fig. 15. Microstructures after corrosion and fatigue studies

Conclusion: The corrosion wear of ferritic - austenitic steels in MACC60 environment was determined, as the samples subjected to corrosion were shown to have reduced durability compared to samples that were not subjected to corrosion. The cracks have a pronounced transcrystalline character, which is explained by the fibrous structure of the samples studied. Welded samples subjected to corrosion have a reduced durability compared to welded samples that are free of corrosion.

B.4.9. Georgiev G., Argirov Y., Mechkarova T., Spasova D., Stoyanova A., Study of the durability of ferritic-austenitic steel samples after cyclical fatigue impact, IOP Conference Series: Materials Science and Engineering, Volume 1037, Issue 1, 11 February 2021 Art. number No 012036, ISSN 17578981, DOI: 10.1088/1757-899X/1037/1/012036

Objective: The purpose of this article is to investigate the fatigue strength of corrosion resistant ferritic austenitic steels used in marine equipment. Two groups of sheet steel samples were prepared: the first group were reference parts and the second group of samples were welded. The fatigue tests were performed with specially developed vibrating equipment. The destroyed surfaces were examined by optical microscopy, and the phase composition by X-ray diffraction analysis. Fatigue strength was evaluated by the number of cycles needed for a crack at a certain alternating load. Fatigue tests show how multi-cyclical fatigue affects the formation and development of a fatigue crack, and metallographic and X-ray diffraction analysis shows the phase changes occurring in the structure of SAF 2507 steel.

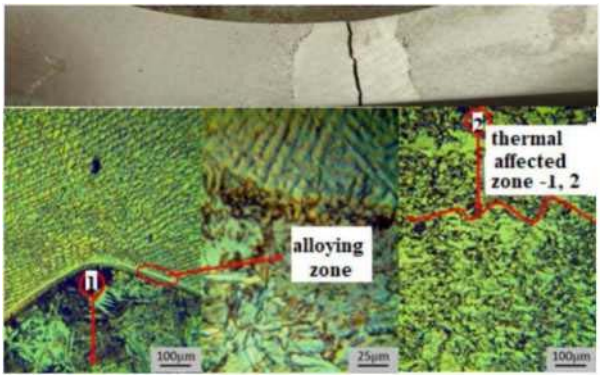

Fig. 16. Microstructures after multicycle fatigue testing

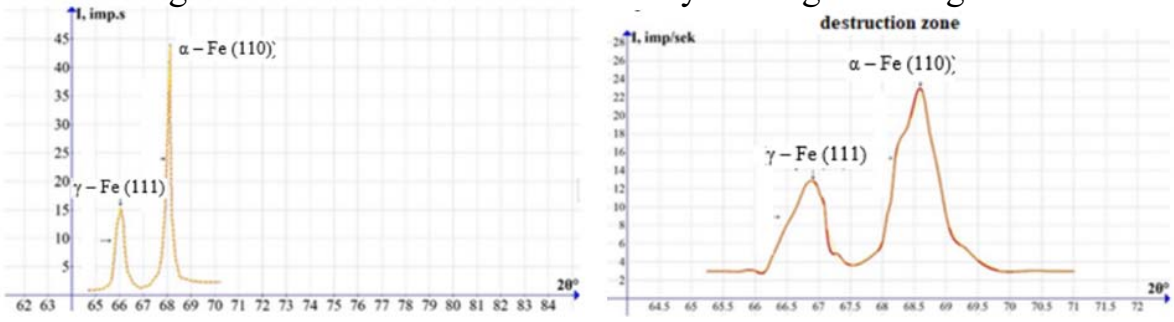

Fig. 17. X-ray phase analysis

Conclusion: An increase in the dislocation density and surface internal stresses of γ-Fe (111) and α- Fe (110) was found from the widening of the X-ray line in the fracture area of the unwelded samples.

B.4.10. Maximov J., Duncheva G., Anchev A., Dunchev V., Argirov Y., Todorov V., Mechkarova T., Effects of Heat Treatment and Severe Surface Plastic Deformation on Mechanical Characteristics, Fatigue, and Wear of Cu-10Al- 5Fe Bronze, Materials, Volume 15, Issue 2, 4 December 2022, Art. number No 8905, ISSN19961944, DOI: 10.3390/ma15248905

Purpose: Aluminium bronzes are widely used in various industries because of their unique properties, a combination of high strength, wear resistance, and corrosion resistance in aggressive environments, including seawater. In this study, the subject of comprehensive experimental research was Cu-10Al-5Fe iron-aluminium bronze (IAB) with β-transformation, received in the form of hot-rolled bars. The effects of different heat treatments (HT) and severe surface plastic deformation (SPD), conducted by diamond burnishing (DB) on the microstructure, surface integrity (SI), mechanical properties, low- and mega-cycle fatigue strength, and dry sliding wear resistance, were determined. Based on quantitative indicators, the applied heat treatments in combination with severe SPD were compared. Thus, the integral efficiency of the heat treatments was evaluated, and the heat treatments were correlated with the resulting properties and operational behaviour of Cu-10Al-5Fe IAB.

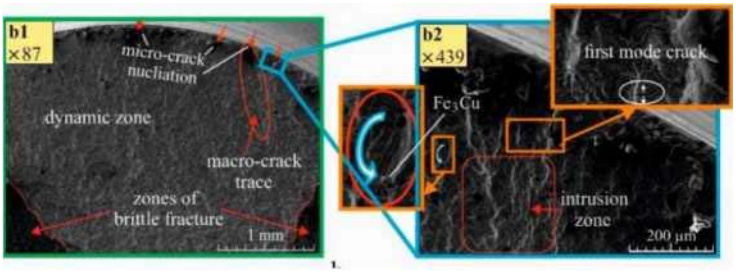

Fig. 18. Fractographic study of fatigue failure

Conclusion: The aim of this article is to quantify the effects of different HTs and severe SPD on the microstructure, SI, tensile strength, impact toughness, hardness, fatigue strength, and dry sliding wear resistance of Cu-10Al-5Fe IAB. An experimental approach was used, including XRD and SEM analyses, an evaluation of the SI obtained after different HTs and DB, tensile tests, impact toughness and hardness tests, rotating cantilever bending fatigue tests, and dry sliding wear resistance tests. Based on the experimental results, a ranking from 1 to 5 was determined for the four different HTs and the as-received condition according to nine criteria with equal relative weights.

B.4.11. Spasova D., Argirov Y., Petrov P., Mechkarova T., Study of the Behavior and the Mechanical Properties of Adhesively Bonded Polymer Matrix Composites Under Mechanical Loading, TEM Journal, Volume 12, Issue 1, Pages 36 - 42, February 2023

Objective: The main aim set in the present work was reduced to the obtaining of PMCs made by adhesive bonding of two composites with a matrix of different types of resin (vinyl ester and epoxy) and the study of their behaviour in determining their mechanical properties. The studies were carried out with four types of adhesively bonded PMCs made in the form of laminates produced from a combination of three types of resin (two types of vinyl ester and one type of epoxy resin) and reinforced with biaxial fiberglass. The aim is to combine the lack of shrinkage of the epoxy resin with the better mechanical properties and better productivity of the vinyl ester resin. An analysis to determine shear strength, tensile strength and bending strength of the investigated composites was made. A macrostructural fractographic analysis to investigate the material behaviour under mechanical loads was carried out.

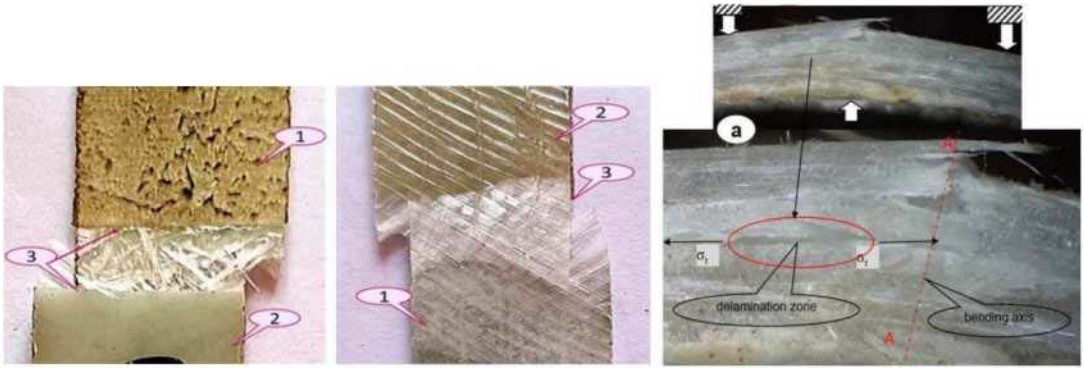

Fig. 19. Fractographic study after tensile and bending tests

Conclusion: Finally, we can conclude that the technology for the fabrication of PMCs, by These types of defects are stress concentrators that significantly reduce the material strength, but this is generally a problem of the composite laminate manufacturing technology (hand contact) and not of the adhesive bonds during bonding laminates of PMCs with a matrix of different types of resin, in which vacuum forming and subsequent manual contact building are combined (which can also achieve the fabrication of complex surfaces), leads to positive results that do not alter the properties of the composite.

Summaries by indicator G.8 - scientific publications in non-refereed reviewed journals or edited collective volumes

G.8.1. Stoyanova A., Bakalova M., Mechkarova T., Simulation thermal analysis to determine the effect of temperature on the surface layer after air-plasma surface cutting., "Mechanical engineering and technologies", NTS, TU-Varna, Issue 2, 2010, 77c, ISSN 1312-0859

Purpose: Investigation of the influence of temperature, thermal cycle and cooling rate during plasma machining on hardness during air-plasma surface cutting process.

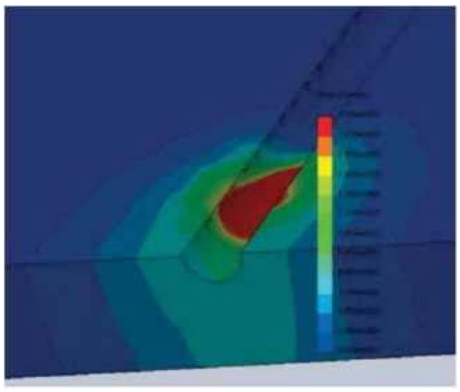

temperature

Table 5

δ, mm	0,25	0,47	0,53	0,82	1,0	1,3	1.42	1,53	1,56	2,0
MHV, kgc/mm-	500	460	520	480	322	300	240	236	220	220

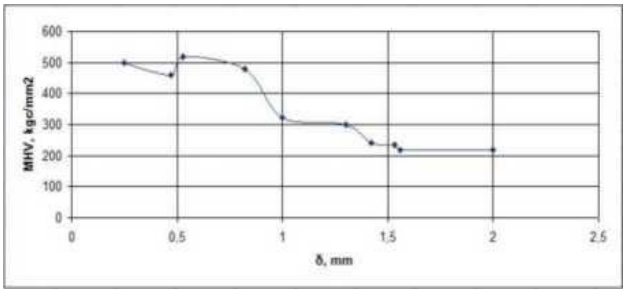

Fig. 20. Experimental data

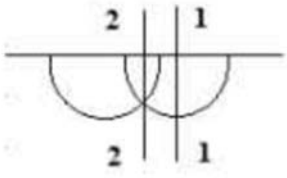

The hardnesses measured after the experiment change constantly in depth.

Conclusion: Comparing the experimental with the simulated c SolidWorks data program shows little discrepancy which does the methodology suitable for future developments and analyses.

G.8.2. Stoyanova A., Bakalova M., Mechkarova T., Avramova T., Methodology for an experimental-statistical study of the relationship between the technological parameters of the air-plasma process cutting., "Mechanical engineering and technologies", NTS, TU-Varna, Issue 2, 2010, 81c, ISSN 1312-0859

Purpose: Experimental-statistical research with the methods of planning the experiment and regression analysis of the relationship between the technological parameters of the air-plasma cutting process.

Table 4: Matrix of the selected plan

№	X_1	X_2	X_3	$X_1 X_2$	$X_1 X_3$	$X_2 X_3$	X_1^2	X_2^2	X_3^3	Y1	Y2	Y3	$\overline{Y}$	Si^2	$\hat{Y}$	$(\overline{Y}-\hat{Y})^2$	Разлика %
1	-1	-1	-1	+1	+1	+1	+1	+1	+1	1,59	1,44	1,56	1,53	0,0063	1,525092	0,00002	2,29
2	+1	-1	-1	-1	-1	+1	+1	+1	+1	1,33	1,36	1,30	1,33	0,0009	1,330214	0,00000	2,27
3	-1	+1	-1	-1	+1	-1	+1	+1	+1	1,07	1,08	1,00	1,05	0,0019	1,05436	0,00002	5,15
4	+1	+1	-1	+1	-1	-1	+1	+1	+1	1,12	1,16	1,20	1,16	0,0016	1,164482	0,00002	3,05
5	-1	-1	+1	+1	-1	-1	+1	+1	+1	1,77	1,74	1,68	1,73	0,0021	1,72755	0,00001	2,75
6	+1	-1	+1	-1	+1	-1	+1	+1	+1	1,02	1,06	1,10	1,06	0,0016	1,057672	0,00001	4,00
7	-1	+1	+1	-1	-1	+1	+1	+1	+1	1,4	1,44	1,45	1,43	0,0007	1,431818	0,00000	1,27
8	+1	+1	+1	+1	+1	+1	+1	+1	+1	1,09	1,1	1,02	1,07	0,0019	1,06694	0,00001	4,40
9	-1,682	0	0	0	0	0	2,829	0	0	1,58	1,6	1,62	1,60	0,0004	1,597023	0,00001	1,44

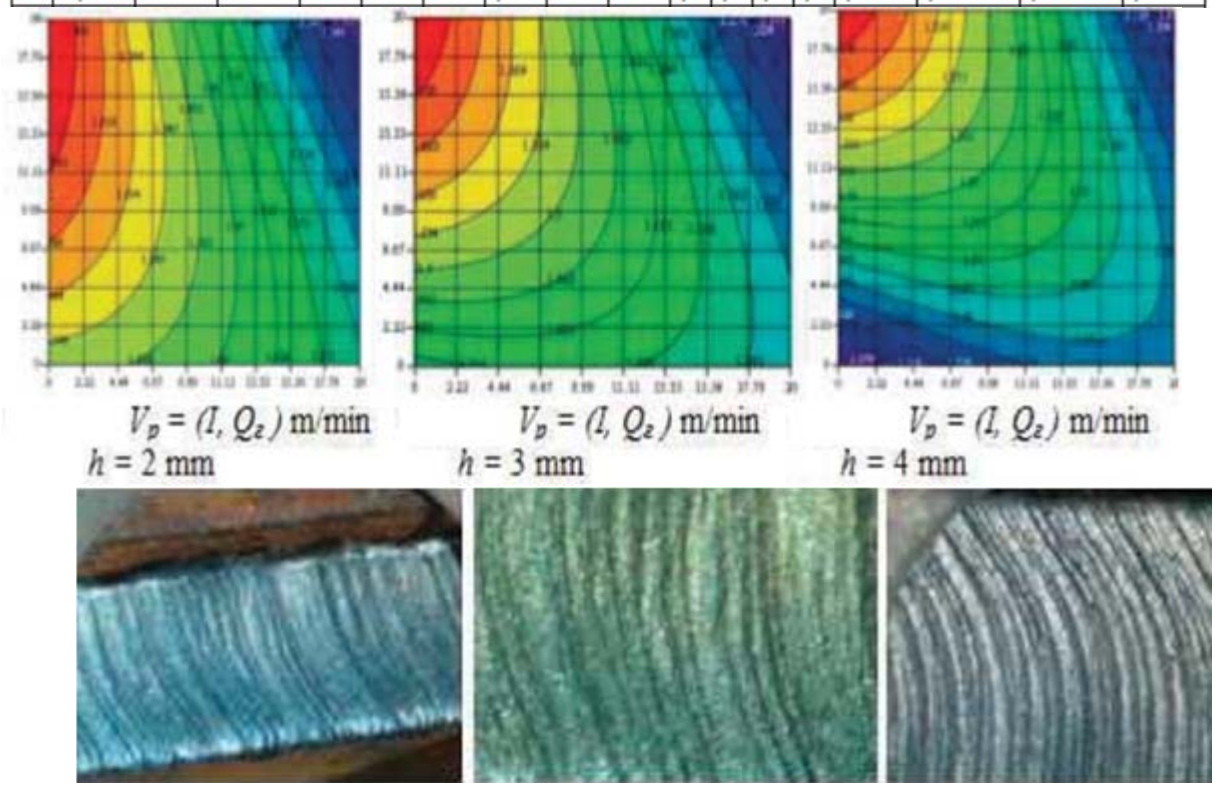

Fig. 21. Macrostructure after air-plasma surface cutting

Conclusion: The most significant factors affecting the quality of surface layers by finding extrema.

G.8.3. Mechkarova T., Stoyanova A., Experimental-statistical study of the technological possibilities of a new kinematic scheme for PPD., XII NTK with international participation, ECOVARNA 2011, 18May 20, 2011, 440 p., ISBN 954-20-00030

Objective: In present article is deduced the relations between kinematical and technological parameters of new scheme for receiving regular relief's of plastic deformation. The present study seeks to optimize the technological possibilities of a new kinematic scheme for PPD by means of multifactorial design experiment statistically treated with the plan of Rechtschaffner. The main factors that are the subject of this study: type and speed of the translational movement of the deforming tool for PPD; revolutions of rotation of the processed shaft; diameter of the deformer spherical element; pressure force, according to preliminary data exert directly influence on the performance of the method and the geometry of the acquisitions microrelief on the processed surface.

Table 5: Matrix of the selected plan

№	X_1	X_2	X_3	$X_1 X$	$X_1 X$	$X_2 X_3$	X_1^2	X_2^2	X_3^3	$\bar{Y}$	Si^2	$\hat{Y}$	$(\bar{Y}-\hat{Y})^2$	Разл%
1	-1	-1	-1	+1	+1	+1	+1	+1	+1	0,5	0	0,550138	0,002513819	9,11
2	+1	-1	-1	-1	-1	+1	+1	+1	+1	0,8	0,0036	0,747174	0,002790586	7,07
3	-1	+1	-1	-1	+1	-1	+1	+1	+1	0,55	0,0007	0,52336	0,00070969	5,09
4	+1	+1	-1	+1	-1	-1	+1	+1	+1	0,7	0,0016	0,680396	0,000384317	2,88
5	-1	-1	+1	+1	-1	-1	+1	+1	+1	0,55	0,0007	0,56031	0,000106296	1,84
...	...	...	...	....	...	...	...	...	...	....	...	...	...	...
20	0	0	0	0	0	0	0	0	0	0,66	0	0,657806	4,814E-06	0,33

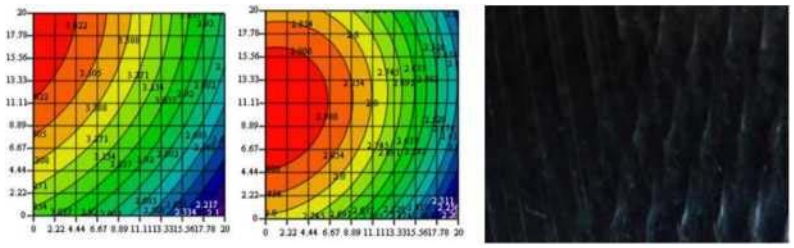

Fig. 22. Experimental statistical research

Conclusion: The most significant factors affecting the quality of surface layers by finding extrema. In the region of the optimum, appearing to him as a local maximum, its importance for roughness after smooth PPD is approximately negligible. Although some of the coordinates of the optimum point are off the limits of the factor space, the influence of the factors on the surface roughness Ra and the trend of the possibilities of its reduction.

G.8.4. Bakalova M., Stoyanova A., Mechkarova T., Simulation roughness study after air-plasma surface cutting., "VII International MTM Congress", Varna, Issue 2, September 19-21, 2011, 53c, ISSN 1310-3946

Purpose: This paper analyses the interconnected impact of the most characteristic parameters of the process on the roughness of the processing and the quality of the produced surface.

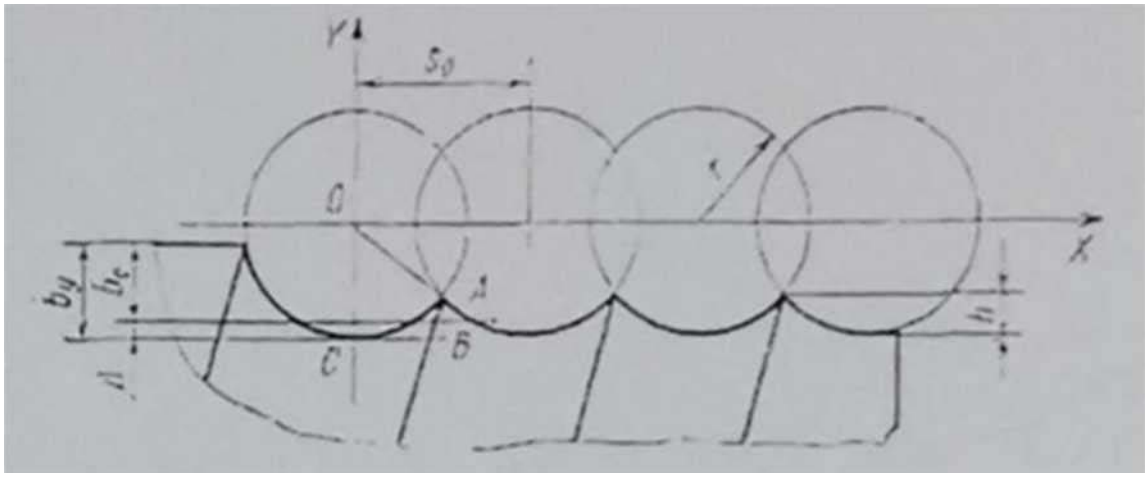

Fig. 23. Kinematic diagram

The maximum penetration depth of the plasma jet can be calculate with the formula:

$$b_c = \frac{0{,}24UI\eta - q_u}{s_0 \upsilon_p \gamma (c_{n1} T_{n1} - c_0 T_0 + c_u)}, \qquad (1)$$

$$h = r - y = r - \sqrt{r^2 - (\frac{S_0}{2})^2}, \qquad (2)$$

Conclusion: With the construction of the geometric model is found analytical relationship between the input geometric parameters (radius of the plasma torch nozzle, center distance of two adjacent locations) and the output geometry parameter the height of roughness-h.

G.8.5. Mechkarova T., Stoyanova A., Methodology for experimental-statistical research of a new kinematic scheme for PPD., "VII International MTM Congress", Varna, Issue 2, September 19-21 2011,53c, ISSN 1310-3946

Objective: In present article is deduced the relations between kinematical and technological parameters of new scheme for receiving regular relief's of plastic deformation . The main objective of the present study is to establish the technological possibilities of the new kinematic scheme for PPD and to optimize the mode parameters experimentally as se use the methods of experiment planning and mathematical statistics. Some of the main factors affecting the performance of the method and the geometry of the resulting microrelief on the machined surface: rate of translational motion of the deforming tool for PPD; revolutions of rotation of the processed shaft; diameter of the deforming spherical element; compressive strength and others. Their influence on the shape and depth of the obtained PMR by the surface layer of cylindrical blanks is multidirectional, which requires their study in an experiential way.

The following are selected as input factors of the plan:

- n- number of coils of the screw line, pcs/l;
- S.l.- step between two adjacent screw lines, mm;
- F- deformation force, kg;

These are the parameters that characterize to the greatest extent the process and directly affect its effectiveness. Except them other confounding factors such as the type and capabilities of the CNC machine, the qualification of the worker, the length of the processed part, the type of material, etc.

Determining the range over which the factors will be varied is related mostly to the possibility of securing independence and compatibility between them, that is why a lower and an upper are set for each factor margin of variation:

Conclusion: Although some of the coordinates of the point of the optima are outside the boundaries of the factor space, it is clearly visible the influence of factors on the surface roughness Ra and the trend of possibilities for its reduction.

G.8.6. Mechkarova T.M., Argirov Y.B., Stoyanova A.M., Research the microhardness of experimental samples after superficial plastic deformation according to a new kinematic scheme to obtain regular microreliefs., "Mechanical engineering and technologies", NTS, TU-Varna, Issue 1, 2012, 31-36c, ISSN 1312-0859

This article presents the outcomes from experimental study of the depth microhardness of new scheme for receiving regular relief's of plastic deformation as well as the variation of the material , microstructure due to applying deformation.

The main objective is to establish through an experimental study the change of the microhardness and the microstructure of the surface the stiffened layer obtained according to a new kinematic scheme for obtaining regular microreliefs by surface plastic deformation.

Task. Bonding the outer surface of a sample with a hardened ball.

Object of research steel C45

Research:

macro-analysis;

microstructural analysis; mechanical characteristics-microhardness hardness HV0.01.

Conclusion:

In all three samples, a decrease in microhardness from the surface layer to the core.

The strengthening is at a depth of up to 0.1mm, which we judge by the values of the measured microhardness - 150 HV0.01, corresponding to the material in delivery status.

Processing conditions significantly affect the microhardness, with the largest influence being the radius of the deforming ball, downforce and feed.

The microstructure corresponds to medium carbon steel and is ferrite- perlite. In the surface deformed zones, a change in the orientation and shape of the grains that grind and follow the direction of deformation.

G.8.7. Mechkarova T.M., Argirov Y.B., Stoyanova A.M., Determination the bearing area and the oil holding capacity of external cylindrical surfaces obtained by surface plastic deformation according to a new kinematic scheme to form a regular microrelief., "Mechanical engineering and technologies", NTS, TU-Varna, Issue 1,2012, 40-44c, ISSN 1312-0859

This article presents the determination support area and oil retention ability of the outer cylindrical surface produced by Plastic deformation surface after a new kinematics scheme for receiving regular relief's.

The main goal is to determine the support through an experimental study area and oil holding capacity of external cylindrical surfaces obtained by a new kinematic scheme for obtaining regular microreliefs by surface plastic deformation.

Task. Hardening the outer surface cylindrical sphere.

Object of research Steel C45

Research:

macro-analysis;

microstructural analysis;

metallographic determination of the obtained relief; mechanical characteristics-microhardness hardness HV0.01.

Conclusion

From the built support curves of the profilograms, it is clear that the best support surface is at Sv.l.=0.4mm; Ra 0.55μm, since the sum is the largest.

When determining the area of the resulting microrelief using "GRAF" program, it is found that the largest oil-retaining area - 1677ym is at an area Sv.l.=0.8mm, when the criterion for roughness is also the largest 9.6%.

G.8.8. Argirov Y., Stoyanova A., Mechkarova T., Influence of the metallurgical defects on the character of destruction at drill pipes., ''Third International Science Congress, 50 years Technical University - Varna", volume 8, 2012, 23-29 p., ISBN 978-95420-0556-8

Target. Inspection of a damaged drill pipe. The object of research is the nature of destruction of a defective borehole pipe with dimensions: D=127 mm; B=9.19 mm according to BDS EN ISO 1455. The material from which the pipe is made is steel grade 135. The manufacturer's certificate includes , the chemical composition and the mechanical properties of steel.

Investigation of object: Determining basic parameters and comparing with these presented by the manufacturer:

macrostructural analysis;

fractographic analysis-observation of the quarry;

microstructural analysis - non-metallic inclusions, metal structure;

mechanical characteristics;

strength testing;

hardness test-HV5;

impact toughness.

Conclusion: A significant amount of pores and non-metallic inclusions were recorded with macro, meso and micro dimensions along both sections of the drill pipe. Presence of surface macropores, with the plastic form, occupying approx. 20 % of the pipe thickness. Presence of pitting corrosion when interacting with the soil primer and the outer surface layer of the tube in operating mode. Active interaction of the dispersed soil primer with the macropores create conditions for the development of a focus of destruction on the outside surface The structure (sorbite, troostite) is homogeneous throughout the section with probability steel to be normalized. Regarding the drill pipe, it can it should be noted that it is characterized by relatively high indicators of relation to the mechanical characteristics. Not always the mechanical ones indicators are the only factor for the working ability of the machine detail. Depending on the working conditions, the influence of the factors change In the case of drilling pipe operation, except for the heavy duty mode load, the influence of the corrosive environment and abrasive and pitting wear depending on the ground primer. Under these working conditions, requires a high degree of purity of the steel in terms of pores, non-metallic inclusions and other metallurgical defects leading to the creation of at the heart of destruction.

G.8.9. Argirov Ya., Stoyanova A., Mechkarova T., Studying the influence of the non-metallic inclusions in the material in fatigue failure of drilling shaft., "Third International Scientific Congress, 50 years Technical University - Varna", volume 8, 2012, 29-34 p., ISBN 978-95420-0556-8

The aim is to study the nature of destruction of a defective borehole shaft shown and the cause of destruction.

Study object: drill shaft, steel grade S 135

Study of the object:

fractographic research - specifying the cause of destruction (malocycle fatigue);
macrostructure;

microstructural analysis-non-metallic inclusions and structure;

mechanical characteristics;

cross-sectional hardness HRC; HRB 5/1000/30;

material strength;

impact toughness.

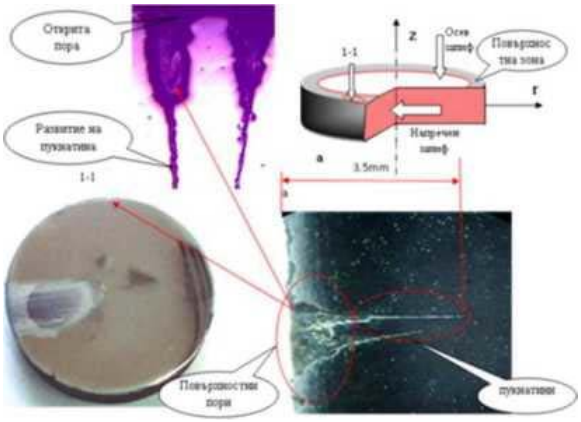

Fig. 24. Research sample

Conclusion: A significant amount of non-metallic inclusions were recorded (oxides) of macro size in the surface layer of the drill shaft.

Presence of surface pores, some of which end with a developed one crack. The total size of the pore with the crack reaches 3.5mm.

From the mechanical tests carried out (hardness, strength, impact toughness) averaged values were obtained: 34.5HRC; 359.6HB5/1000/30; RP0.2=1075.3 N/mm2; Rm=1199.4 N/mm2; A= 16.7%; KCV=35.4 J/cm2. The obtained tensile strength of the tested sample falls within the lower limit of the requirements under BDS EN ISO 898-1 for strength class 12.9. The non-uniform Rockwell hardness (C) in the surface zone is due to the presence of macro non-metallic inclusions. The presence of macro non-metallic inclusions and open metallurgical pores ending in sharp shapes and significant dimensions are the ideal concentrators for the emergence and development of tired zone.

D.8.10. Stoyanova A., Tsoneva Z., Mechkarova T., Research the processes of surface strength hardening of steel 45 by use of concentrated heat sources., ., "Transport, ecology - sustainable development", XX NTC with international participation, EKOVARNA 2014, May 15-17, 2014, ISBN 954-20-00030

Purpose: In the present work, the possibility of plasma is considered surface treatment of one of the most commonly used in the practice iron-carbon alloys, namely steel 45 (C45 according to BDS EN ISO 14556) [1,2].
The possibility of providing the same or improved ones is being considered performance compared to other surface methods strength treatment.

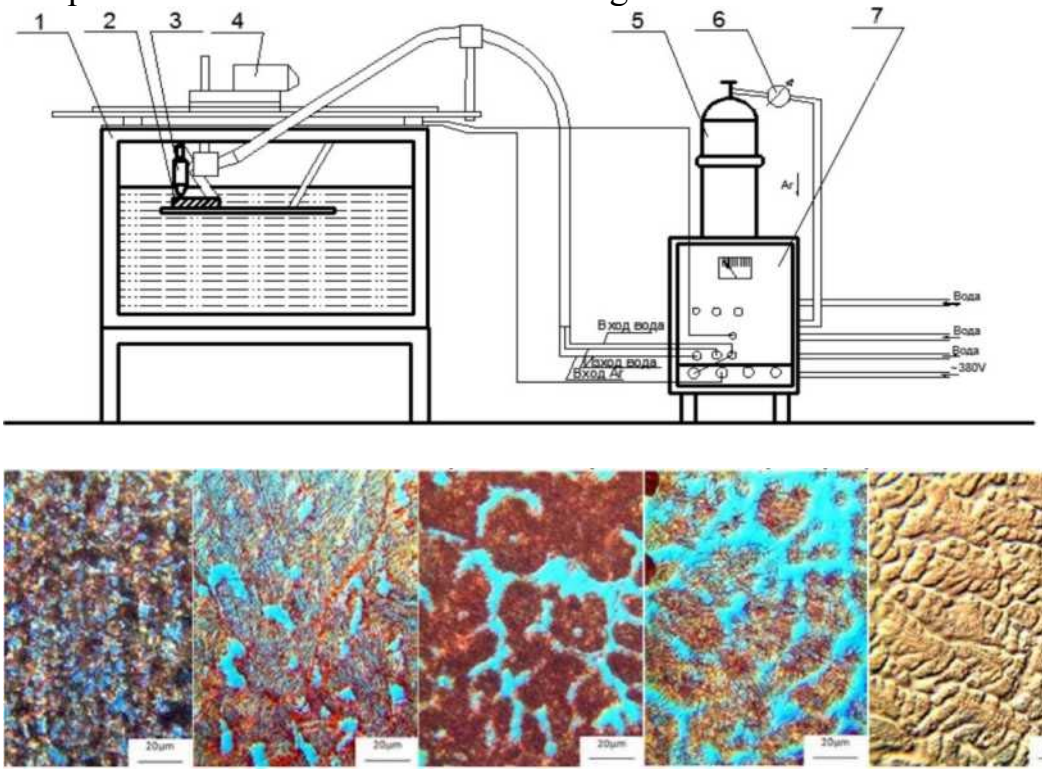

Fig. 25. Structures after plasma surface heat treatment with magnification X500

Conclusion: From the set criterion for evaluating the obtained layers it can be concluded that the surface plasma treatment under a layer of water (with and without additional cooling) has the following advantages over that carried out dry:
- increased hardness of the machined surface with the same other terms;
- greater depth of the strengthened zone;
- smaller zone of thermal influence.

D.8.11. Stoyanova A., Tsoneva Z., Mechkarova T., Experimental- statistical study of the optimal regimes for working under water and dry during surface plasma heat treatment., ., "Transport, ecology - sustainable development", XX NTK with international participation, EKOVARNA 2014, May 15-17, 2014, ISBN 954-20-00030

The aim is to establish the technological possibilities of the method for surface plasma treatment using planning methods of the experiment and mathematical statistics to optimize the modes experimental parameters and creation of new methods and tools, ensuring the increase in quality and productivity the process.

Table 6: Matrix of the selected plan

№	X_1	Z_1 A	X_2	Z_2 m/h	X_3	Z_3 mm	X_1X_2	X_1X_3	X_2X_3	X_1^2	X_2^2	X_3^2	y_1	y_2	y_3
1	-1	100	-1	9,4	-1	5	+1	+1	+1	+1	+1	+1	312	572	602
2	-1	100	+1	19,4	+1	9	-1	-1	+1	+1	+1	+1	260	440	560
3	+1	120	-1	9,4	+1	9	-1	+1	-1	+1	+1	+1	452	591	650

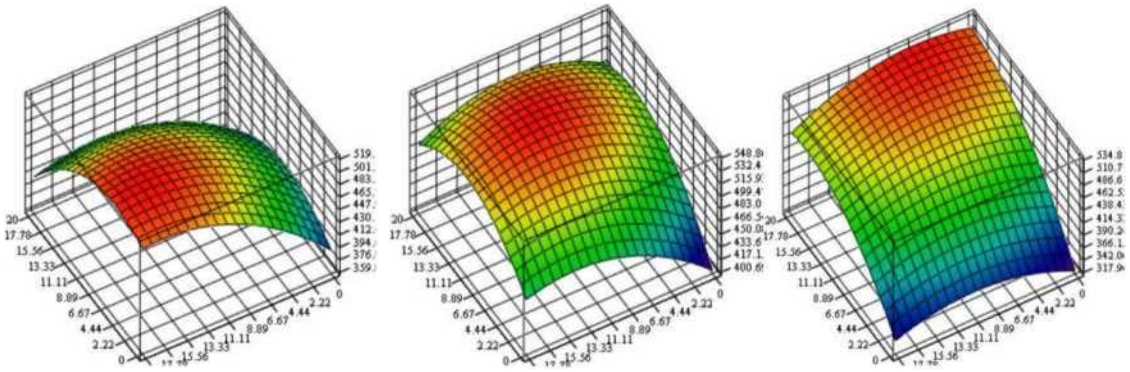

Fig. 26. Isolines showing the variation of the microhardness HV0.05

Conclusion: Analyzing the results obtained in the selected limits of variation of the factors seen as the most influential factor on the microhardness of C45 is the speed of movement of the burner. This is explained by the change in the amount of thermal energy supplied to the surface of the sample under the processing conditions. Except that, the speed of moving the burner also affects the stability of the rainbow burning under water. The depth of the reinforced layer of C45 under water is greater by 1.4 - 1.6 mm than dry, which is due to the additional contraction of the arc by the hydrostatic pressure of the water.

G.8.12. Tatiana Mechkarova, Study of the abrasive wear resistance after manual electric arc welding of samples from steel DD11, Mechanical engineering and technologies, ISSN 13120859, pp. 30-34, 2017

Purpose: In the article, a study of abrasive wear of samples of low-carbon steel brand yy15 welded with three types electrode brand ABRADUR.

The chemical composition of the electrodes is shown in table 1

		C	Cr	Nb	Mo	W	V	HRC
1	ABRADUR64	6,0	26,0	7,5	-	-	-	64
2	ABRADUR65	4,3	9,5	-	2,0	-	-	65
3	ABRADUR66	6,0	22,0	6,0	6,0	2,0	1,0	66

To fulfill the purpose of the study, determining wear resistance of the welded metal, a single-phase wear stand was built electric motor, and the wearing element is a counterbody wrapped with water sandpaper.

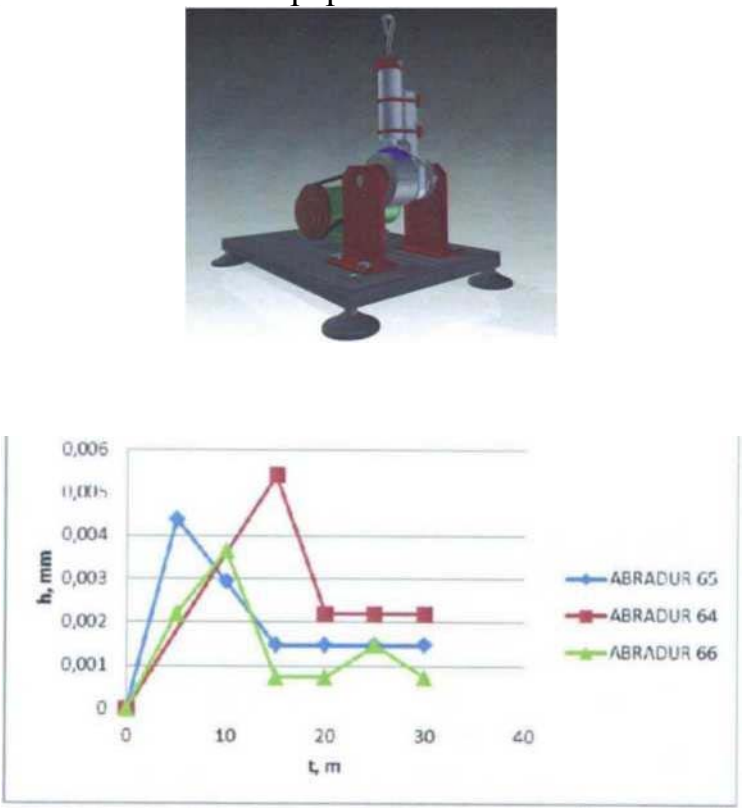

Fig.27 Wear stand and wear resistance results

Conclusion: After the research done, it was found that the best wear resistance over time shows the sample welded with an electrode ABRADUR 64.

G.8.13. Tatiana Mechkarova, Simulation modeling of the processes of the stressed and deformed state in manual electric arc welding, Mechanical engineering and technologies, ISSN 1312-0859, pp. 23-29, 2017

Purpose: The article examines heat exchange processes and tensile deformation load during welding of samples from low carbon steel brand St15 welded with electrode brand ABRADUR64. A computer was used to solve the present task a SolidWorks simulation program with which stresses and deformations in the entire volume of the modeled three-dimensional welded specimen body.

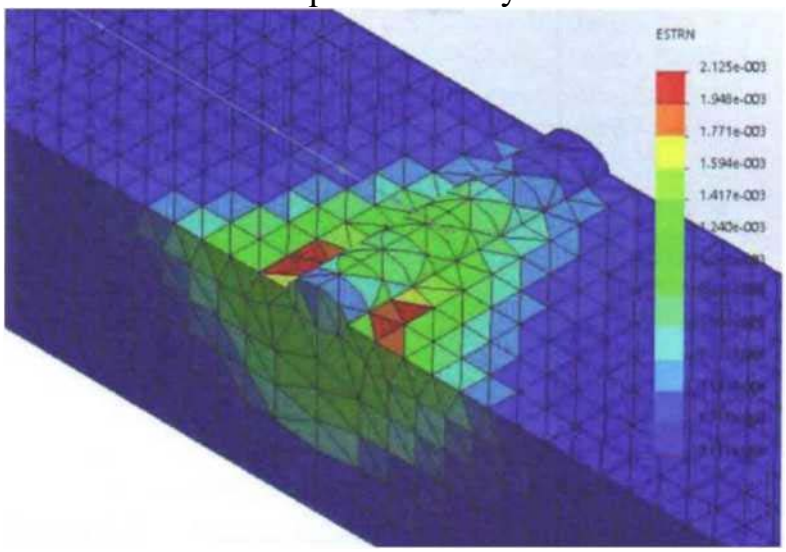

Fig. 28. Results of the computerized SolidWorks program simulation analysis.

Heating simulation

Sensors	Stress	Displacement	Deformation
1	2,64E+08	0,035	9,41E-04
2	2,54E+08	0,034	8,05E-04
3	1,76E+08	0,032	7,71E-04
4	9,96E+07	0,029	3,21E-04
5	2,83E+07	0,026	1,22E-04
6	1,26E+07	0,02	4,81E-05
7	1,39E+07	0,014	5,33E-05

Cooling simulation

Sensors	Stress	Displacement	Deformation
1	4,14E+07	0,013	1,57E-04
2	3,89E+07	0,013	1,33E-04
3	3,51E+07	0,012	1,35E-04
4	3,07E+07	0,011	1,04E-04
5	1,80E+07	0,01	7,07E-05
6	8,10E+06	0,007	3,08E-05
7	8,66E+06	0,005	3,38E-05

Conclusion: The determination of the maximum total deformations in welded structures is essential to solve the problems of the accuracy during their installation.

In the cooling process, the largest stresses are grouped in the deposition zone, which is explained by their different coefficients of thermal expansion and various mechanical properties.

G.8.14. Tatiana Mechkarova, Studying the structure of surface welded layers with ABRADUR66 on low carbon steel, Union Notices of scientists-Varna, Series "Technical Sciences" - 1'2017, ISSN 1310-5833, pp. 51-54

Purpose: Research welding process with ABRADUR 66 electrode on low carbon steel DD11, which is preheated to 200 degrees to avoid the formation of cold cracks.

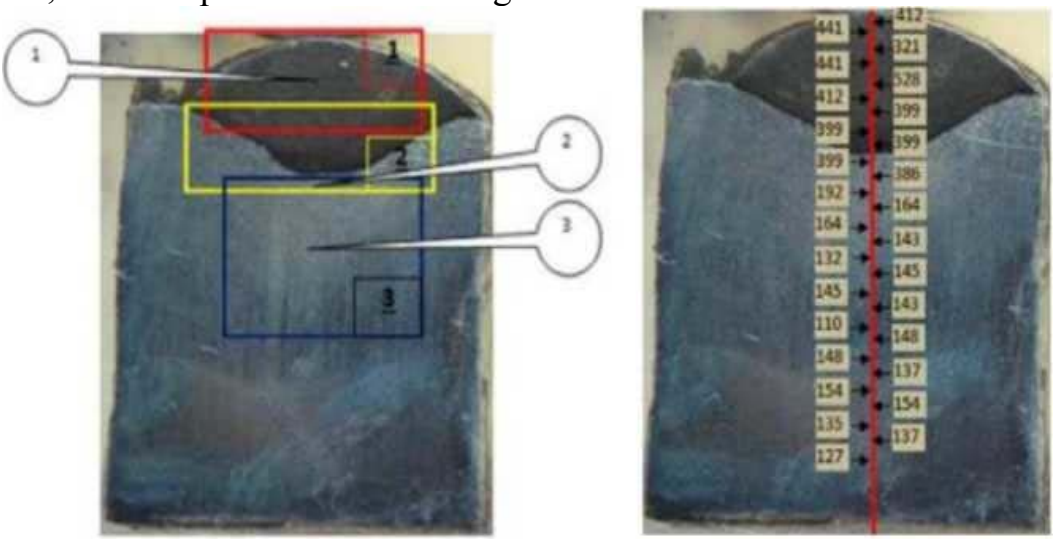

Fig. 29. Macro structure of the boiled compound, measured micro Vickers hardness HV0.05

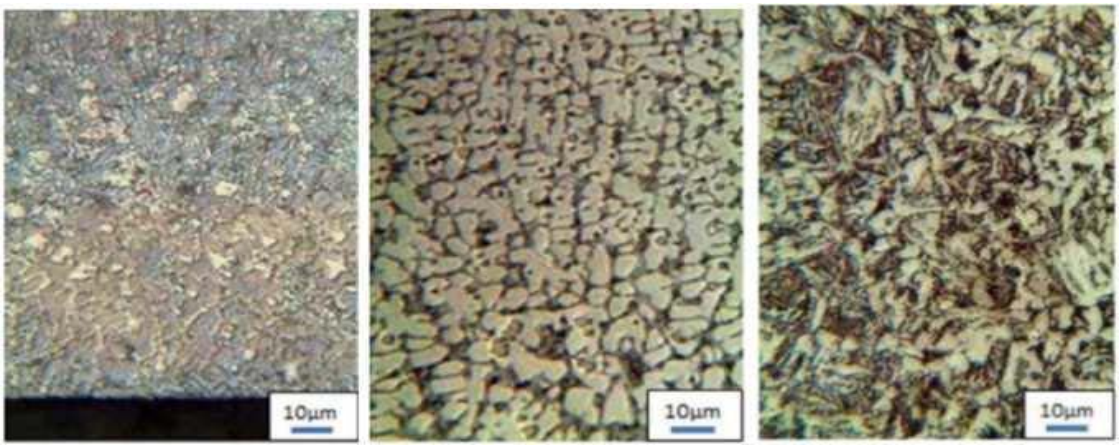

Fig. 30. Microstructures in welded metal, zone of thermal influence and base metal

Conclusion: In the different areas of the macrostructure of the studied test body (welded metal, thermally affected zone, base metal) se observed inhomogeneity in structure and hardness. In the uppermost layers of inhomogeneous acicular martensite and residual are observed in the welded metal austenite. Towards the fusion limit, the structure becomes residual austenite and troostite. This is evidenced by the growth of the microhardness in the welded metal layer. A carbide phase has formed there located preferentially on the boundaries between dendritic crystals.

G.8.15. Tatyana Mechkarova, Structural changes during manual arc welding with ABRADUR64 electrodes, Notices of Union of Scientists-Varna, "Technical Sciences" Series - 1'2017, ISSN 1310-5833, p.47-50

Objective: Analysis of structure and properties of boiled samples from low carbon steel DD11 with ABRADUR 64 electrode. The structure is examined with a metallographic microscope, which is equipped with an attachment for HANEMAN Vickers microhardness test

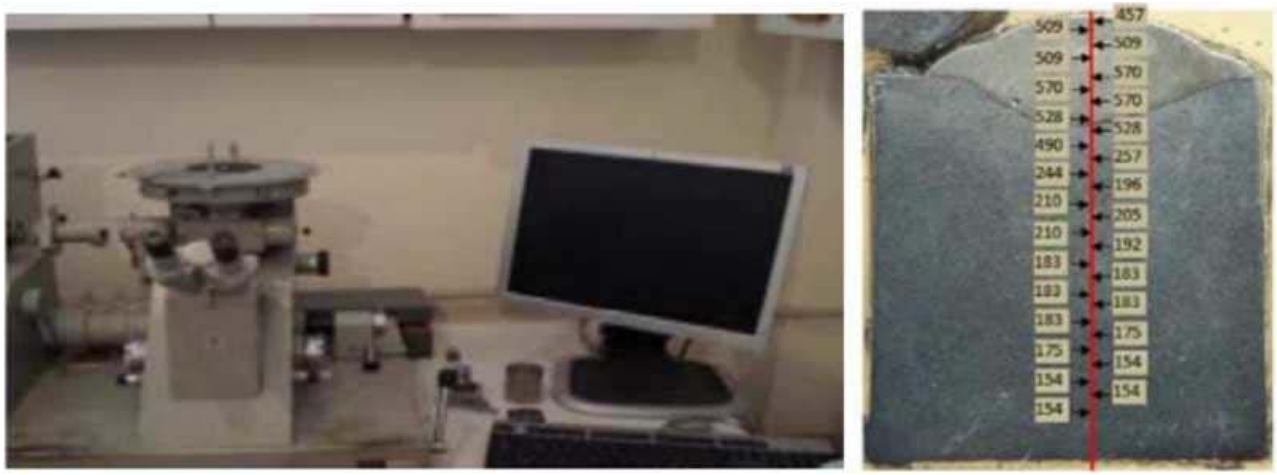

Fig. 31. Metallographic microscope with attachment for measuring Vickers microhardness HV0.05 and the measured hardnesses in transverse section

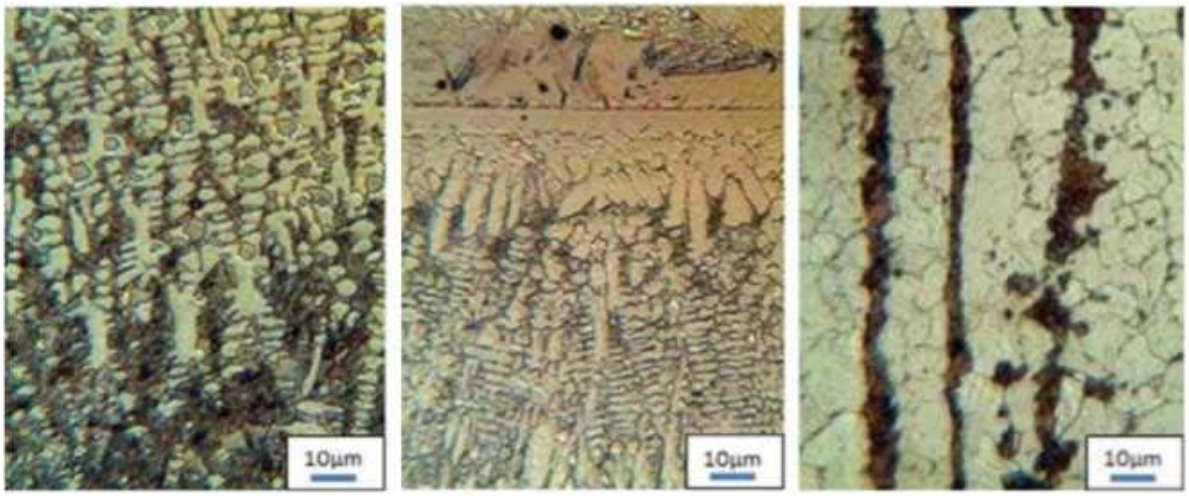

Fig. 32. Microstructures in welded metal, alloying limit and base metal

Conclusion: In the zone of the welded metal there is a pronounced dendritic structure. The alloyed electrode material leads to a strengthening of the the welded surface. A significant amount is released at the borders carbides. In the zone of thermal influence, the structure is finely divided ferrite- pearlitic, which is also characteristic of the base metal.

D.8.16. Georgiev G., Argirov Y., Mechkarova T., Antonov G., Modeling of shaft - weel from centrifugal pump made of duplex steel SAF2507 and simulation of strain and fatigue curve, International Journal "NDT Days 2017", ISSN 1310-3946, pp. 254-257

Purpose: The object of research is a computer simulation analysis of fatigue strength of SAF2507 duplex steel and comparing the obtained results with experimental ones. In SolidWorks program it is created three-dimensional model of a pump shaft-impeller.

Stages of performing the simulation:

• First step: setting restrictions (strengthening in support surfaces) in the movement of the shaft with the impeller in the bearings;

• Second step: setting the speed of rotation of the shaft, 2900 revolutions in minute;

•Third step: Enter working parameters: 130 N per workpiece with direction reverse of shaft rotation;

•Fourth step: setting the material of the model: steel 1.4410 (SAF2507);

•Fifth step: entering the experimental data and constructing the SN curve necessary for the simulation in the case of fatigue of the material;

• Sixth step: Selection of operating mode parameters when simulating the cyclic load and symmetrical cycle LR = -1;

• Seventh step: running the simulation and getting results for stresses, strains, fatigue strength, etc.

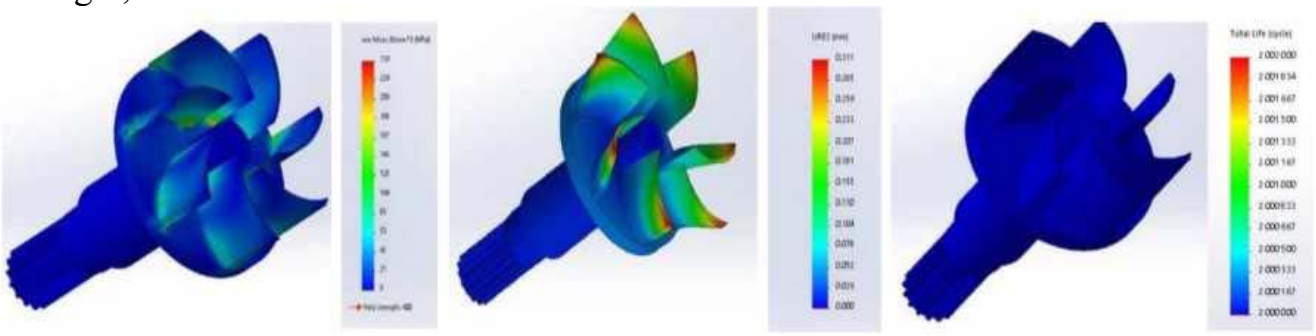

Fig. 33. Results for stresses, strains and number of cycles

Conclusion: In the experimental research done for tired strength of the studied material of duplex steel brand SAF2507 se found that the critical cycles for fatigue failure to occur are at the order of 250,000 cycles at a set voltage of 332 MPa. After the performed simulation makes it clear that dangerous zones are only those in the thinnest parts of the blades of the impeller in their support zone.

G.8.17. Stoyanova A., Mechkarova T., Yordanov K., Study of the influence of the technological parameters of the air-plasma surface gouging on some quality characteristics in the surface layer, Annual Journal of Technical University of Varna, Vol. 1 Issue 1 (2017), ISSN: 2603-316X (Online), pp 105-111, DOI: 10.29114/ajtuv.vol1.iss1.29

Objective: The efficient use of resources on the basis of the development of scientific and technical progress requires widespread implementation of new technologies for processing of metals, such as plasma, cathode-ray, detonation and other methods that allow to increase the lifetime of machines operation and reduce the materials and energy consumption throughout production.

The aim of this paper is to investigate the relation between the technological parameters of the process air-plasma surface gouging and the quality characteristics of the obtained surface layers.

The relations between technological parameters of the process air-plasma surface gouging of metals and quality parameters were obtained by using rotatable design of experiments and regression analyses techniques.

Table.12. Matrix with the factors (X1,2,3) that vary and the response (Y1,2,3,4)

№	X_1	X_2	X_3	$X_1.X_2$	$X_1.X_3$	$X_2.X_3$	X_1^2	X_2^2	X_3^3	Y1	Y2	Y3	Y4
1	-1	-1	-1	1	1	1	1	1	1	502	605	152	2,09
2	1	-1	-1	-1	-1	1	1	1	1	480	583	130	1,83
3	-1	1	-1	-1	1	-1	1	1	1	450	553	100	1,57
4	1	1	-1	1	-1	-1	1	1	1	445	548	95	1,62
5	-1	-1	1	1	-1	-1	1	1	1	470	573	120	2,27
6	1	-1	1	-1	1	-1	1	1	1	430	533	80	1,52
7	-1	1	1	-1	-1	1	1	1	1	509	612	159	1.90

$$Y1\,(X1, X2, X3) = 499.216867 - 16.878864*X1 - 5.145890*X2 - 1.950394*X3 - 10.500000*X1*X3 + + 16.750000*X2*X3 - 10.443885*X1*X1 - 12.742548*X2*X2 - 8.498862*X3*X3 \quad (3)$$

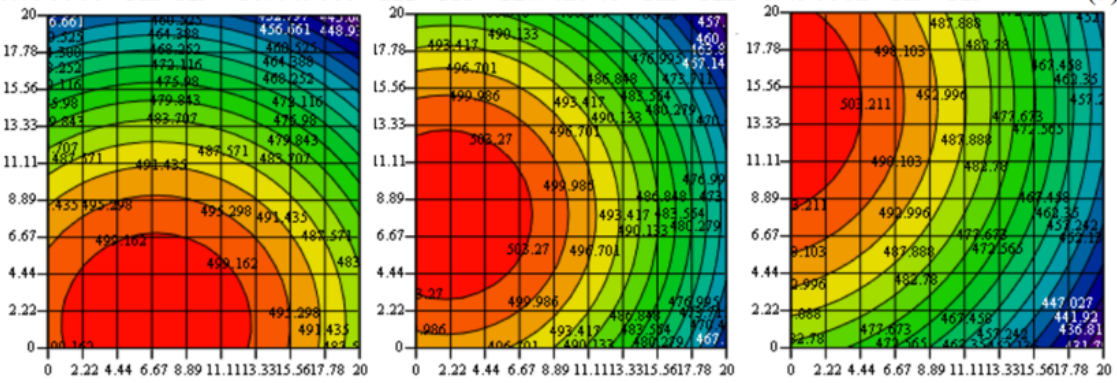

a) HV5 = (h, I) when Vp = 1,4 m/min

b) HV5 = (h, I) when Vp = 1,5 m/min

c) HV5 = (h, I) when Vp = 1,6 m/min

G.8.18. Mechkarova T., Argirov Y., Antonov G., Stoyanova A., Hot Forging Computer Simulation of Tee from Steel 16Mo3, International Journal "NDT Days", Volume I, Issue 4, Year 2018, eISSN: 2603-4646, pp. 544-550

Bonding of industrial installations involves the use of pipelines that are not always in a straight line, and the use is required of deviations, which are carried out with so-called tees. When fluid is superheated steam and pressure 40 bar tees are hot stamped and from heat-resistant steels, for example steel 16Mo3, which acc specification and has the required chemical composition and mechanical characteristics.

The purpose of this paper is a computer simulation analysis of stresses, strains and strain rates in hot stamping in a specialized Q-Form program on a 16Mo3 steel tee.

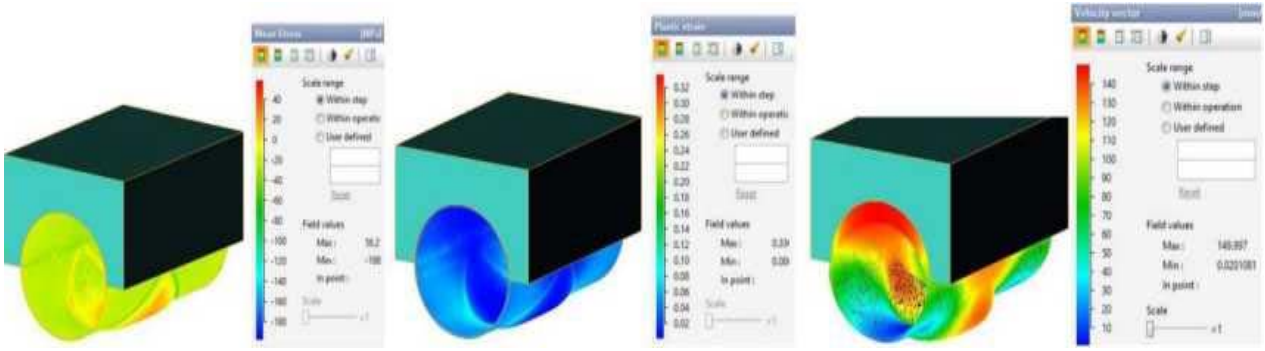

Fig. 35. Results of a computer simulation analysis of stresses, strains and strain rates with the Q-Form program After the simulation analysis, the following data were established for obtained stresses and deformations in the deformed workpiece:

- reported maximum stresses: 58 MPa;
-maximum plastic deformations: 45mm;
-maximum speeds: 150mm/s.

After the computer analysis, a complex analysis can be made evaluation of the effectiveness of the use of simulation 3D programs as a QForm to get an unlimited number of predicted results for real hot stamping process, which is cost-effective, so thus saving the expenditure of additional funds from real trials. The obtained results for stresses, strains and velocities from simulation analysis are apparently adequate and allow the application of the software in solving real engineering tasks.

G.8.19. Tatyana M. Mechkarova, Krastin K. Yordanov, Semi-automatic MAG welding of alloyed machine-building steels, Power Transmissions'19 Proceedings, Vol. 3, ISBN: 978-619-7383-12-6, pp. 419-422, 2019

Purpose: Object of research is experimental statistical study by regression models of a three-factor experiment (Rechtschaffner) when studying the significance of factors that are regime process parameters semi-automatic MAG welding of three steels with carbon equivalent 0.4%, 0.5% and 0.6%.

Item	Steel grade	Chemical elements, %										Carbon equivalent
	EN10027-1	C	Si	Mn	Cr	Ni	Mo	V	Cu	S	P	C_{eq}, %
1.	X60	0,140	0,29	1,42	0,010	0,020	0,030	0,08	-	0,006	0,010	0,40
2.	S460N	0,159	0,33	1,54	0,031	0,599	0,013	0,16	0,02	0,005	0,010	0,50
3.	S960QL	0,150	0,47	1,31	0,545	0,787	0,318	0,04	0,04	0,003	0,010	0,60

Item	Steel grade	Yield limit, Re [MPa]	Tensile strength, Rm [MPa]	Relative elongation, A_5 [%]
1.	X60	440	500÷680	17
2.	S460N	460	520÷700	16
3.	S960QL	960	1000÷1300	12

The mode parameters of the process are:

-DC+

- I=12-220A

-U=18-35V;

-wire output speed V=5.5-5.7m/h

-gas consumption Q=15-18dm3/min

-electrode material OKAutRod12.51

Regression equation:

$$y = 465,16 + 75,24 \cdot \chi_1 + 83,74x_i + 18,99x_3 + 13,79\text{-}x_r x_i + 14.54x_2x_3\text{-}4,91x_yx_1 + 12,03\, x_i^j \text{-}36.47\text{-}X1^2 + 16.28\text{-}x,\cdot$$

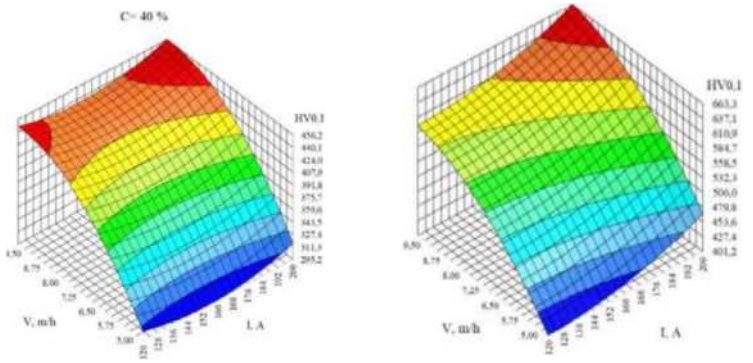

Fig. 36. Graphical results for the extremum

G.8.20. Konsulova-Bakalova M., Mechkarova T., A study of strength properties of welded copper plates and determining the crusher zone, Conference: 6th International Bapt Conference, Power Transmissions'19at: Varna, Bulgaria, ISBN: 978-619-7383-12 -6, Volume: III, pp. 423-426, 2019

Purpose: This article presents a study of the thermal processes and stress deformation state in copper welding thin plates by TIG method.

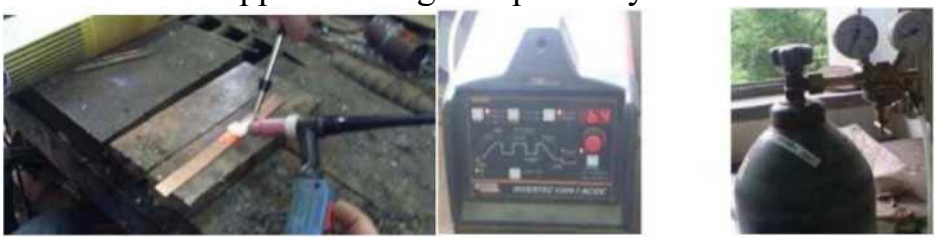

Fig. 37. Installation for TIG welding

Mode parameters:

-Current: I=55A; 60A;85A

- Consumption of protective gas argon:12-14 l/min;

A mechanical tensile strength test was performed on the welded plates

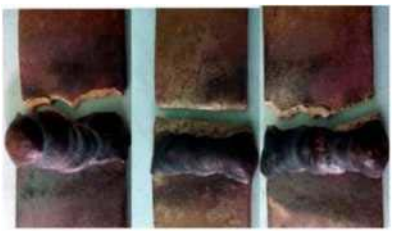

Current	I=55A	I=60A	1=85A
Rm (MPa)	164	186	144
A(%)	14.1	26.0	18.7

Fig. 38. Tensile strength of welded copper plates

During the research, a computer simulation analysis was also carried out in SolidWorks program of temperature distribution and determination of stresses and strains.

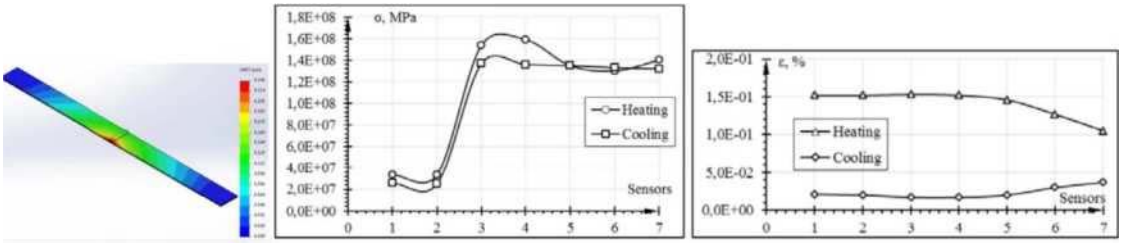

Fig. 39. Computer simulation analysis of stresses and strains

Conclusion: From the analyzes made, it can be concluded that the best mechanical performance is given by the mode with 60A current.

G8.21. Mechkarova T., Stoyanova A., Antonov G., Exploring the Technological Possibilities for 3d Scanning and Computer Simulation of Forging Gears from Steel 45, International Journal "NDT Days", Volume II, Issue 4, Year 2019, eISSN: 2603-4646 , pp. 489-494

Purpose: This article presents a methodology for volume 3D scanning and building a computer simulation model of stamped 45 steel gears.

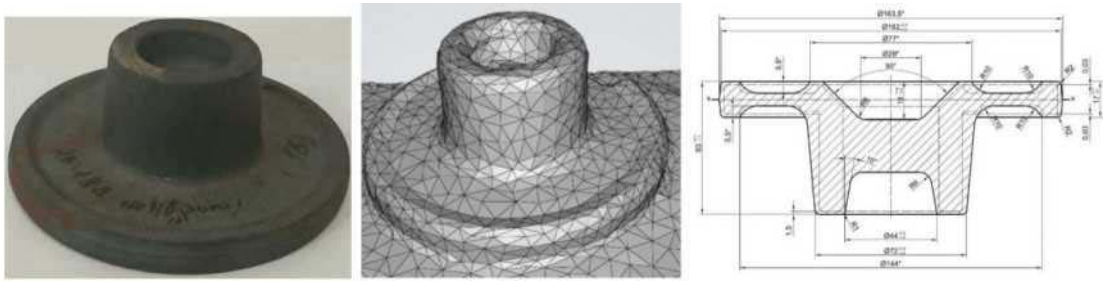

Fig. 40. Real object gear stamping and scanned model on the basis of which a drawing of the forging is prepared. 3D

Stages of performing a computer simulation of a hot process stamping with QForm software product.

-Introduction of the tools and the cylindrical workpiece generated with the AutoCAD program in the drawing field of the QForm program.

- Selection of boundary conditions in QForm program consisting of: the materials of the workpiece and tools, temperature of the preheated billet and initial temperature of the tools, type of stamping press and stamping

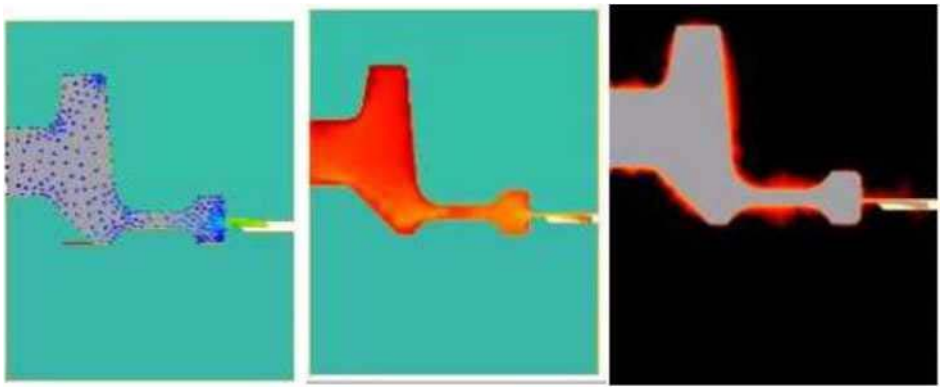

Fig. 41. Results for velocities, temperatures, stresses and strains

Conclusion: Computer simulation analysis allows for simulation study of real plastic flow processes of metal and stress distribution during hot process plastic deformation.

D.8.22. Aneliya Stoyanova, Tatyana Mechkarova, Mariya Konsulova-Bakalova, Krastin Yordanov, Underwater Twin-Arc Gas Metal Arc Welding for Low-Alloy Shipbuilding Steel, Indian Journal of Production and Thermal Engineering (IJPTE), ISSN: 2582-8029(Online), Volume -1 Issue-1, December 2020, Published By: Lattice Science Publication (LSP), Journal Website: www.ijpte.latticescipub.com, pp.7-12

Objective: The present work determines the impact of some of the main factors influencing the quality of the welding joint during underwater welding in gas metal arc welding (GMAW) with two arcs supplied by two power sources. The variables chosen are: the alteration of the currents in the welding arcs, the distance between the arcs and the welding speed. The problem is solved by mathematical planning of the experiment whereby the optimization parameter is the hardness in the zone of thermal influence.

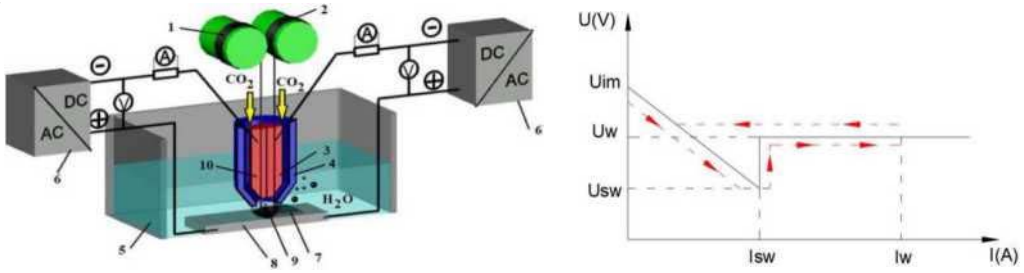

Fig. 33. Schematic of the experimental setup and VA characteristic.

The chosen design was a three-factor regression analysis.

Factors (levels of alteration)	Coefficient Xo	Distance between electrode wires, S, mm	Velocity of welding, V_s, m/h
	Xi	Xi	Xi
Basic level; xo	0.53	18	11
Interval of alteration; Ax	0,01	2	2.5
Top level; xi=+l; i=1.2	0.54	20	13.5
Bottom level: XF-1; s=1.2	0.52	16	8.5

№ of tests n	Factors (levels of alteration)										Y1	Y'	Y,	Y
	Xo	Xi	Xz	Xs	ХД	Xr-Xs	Xi-Xs	X?	X?	X?	Optimization parameter, HV5			
1	1	-1	-1	-1	1	1	1	1	1	1	287	286	282	285
2	1	-1	1	1	-1	-1	1	1	1	1	305	304	300	303
3	1	1	-1	1	-1	1	-1	1	1	1	282	281	277	280
4	1	1	1	-1	1	-1	-1	1	1	1	288	287	283	286
5	1	-1	-1	1	1	-1	-1	1	1	1	292	291	287	290

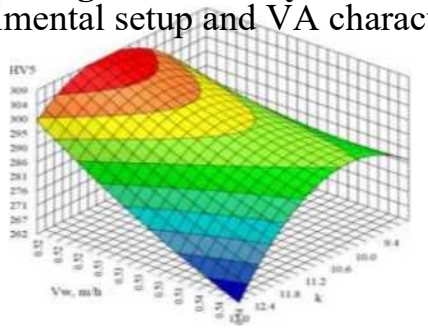

Fig. 42. Graphic representation of the extreme

Conclusion: The performance and interpretation of linear regression analysis are subject to a variety of pitfalls, which are discussed here in detail. The reader is made aware of common errors of interpretation through practical examples. Both the opportunities for applying linear regression analysis and its limitations are presented.

G 8.23. Aneliya Stoyanova, Tatyana Mechkarova, Mariya Konsulova-Bakalova, Krastin Yordanov, Investigating Heat Transfer of Manual Metal Arc Hard facing of Low Carbon Plates, Indian Journal of Production and Thermal Engineering (IJPTE), ISSN: 2582-8029(Online), Volume- 1 Issue-1, December 2020, Published By: Lattice Science Publication (LSP), Journal Website: www.ijpte.latticescipub.com, pp.1-6

Purpose: This study presents the results of a computer simulation study of thermal processes in low-carbon Manual Metal Arc (MMA) hardfacing plates with E DUR600. The problems related to the thermal processes occurring during the heating of sheets of steel DD11, manual metal arc hardfacing with electrodes E DUR600, by examining the influence of temperatures, the heating time and the geometry of the test plates. By computer simulation using SolidWorks software, which have Finite Element Analysis (FEA) engineering systems resulting in simulations of temperature distribution over time and the direction of heat fluxes in the thermal influence zone after the MMA hardfacing process.

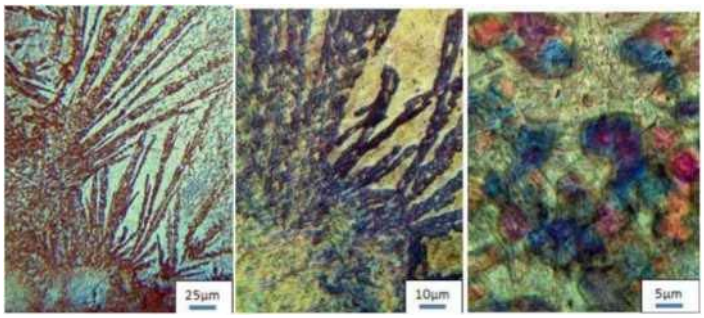

Fig. 44. Microstructures of the welded samples

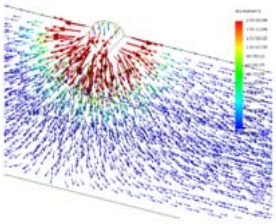

, τ [s]	3	6	9	12	15	18	30	90
q_{max}, [W/m^2]	26 000	95 000	541 000	1 198 000	1 479 500	3 442 028	5833,3	1456,5
q_{min}, [W/m^2]	2,270	2,343	2,703	3,500	4,597	7,658	2,875	5,266

Fig. 43. Results for the magnitude of the heat flow

Conclusion: From the micro-structures in Figure 3 it is evident that there are no cracks, non-metallic inclusions, undercuts and other defects at the boundary of alloying or in the eld metal.

D.8.24. Mechkarova T., Argirov Y., Atanasov N., Stoyanova A., Cold Forging Computer Simulation of Bushing from Steel GX120Mn13, International Journal "NDT Days", Volume III, Issue 2, Year 2020, eISSN: 2603-4646, pp. 104-109

Purpose: The article presents a simulation deformation analysis of process cold plastic deformation of a sleeve from high alloy manganese steel GX120Mn13.

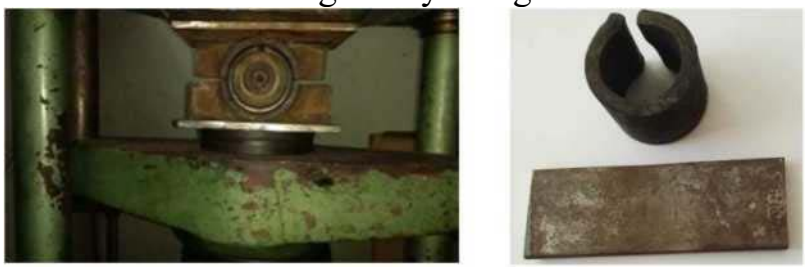

Fig. 45. Experimental stand

To perform the computer simulation analysis are used the capabilities of software for modeling metalworking processes DeForm-F23.

First step: Selection of specimen material and matrix plates.
- material of the matrix plates and the punch L6(ASTM)
- material of the workpiece: GX120Mn13(DIN EN 10349);

Step two: enter operating temperatures.
- workpiece temperature: 20oC;

Third step: input mode of operation.
- the lower matrix is set to be stationary;
- hydraulic press is selected: 120MN;

Step Four: Start the simulation and get the results for: stresses, strains, velocities.

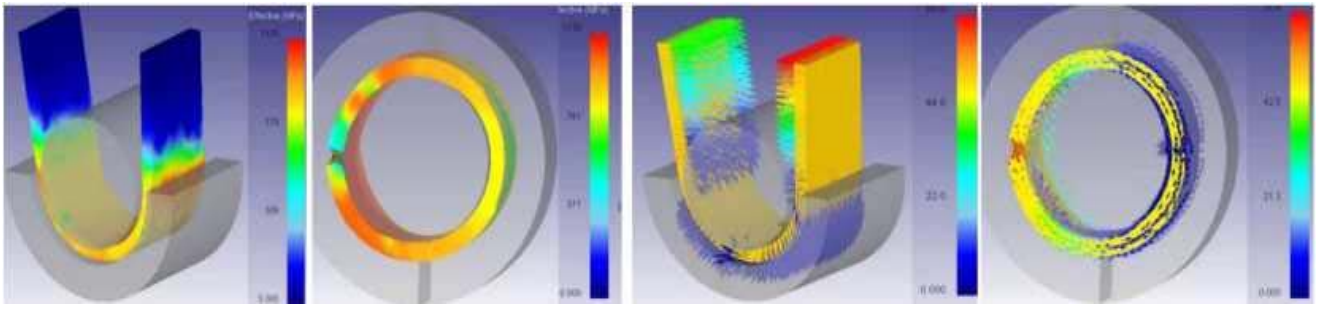

Fig. 46. Simulative analysis in DeForm-F23

Conclusion: The obtained results for stresses, strains and velocities from the simulation analysis are below the limit values for crack initiation for this material GX120Mn13 (DIN EN 10349), which means that they are adequate and allow their application in real processes of cold plastic deformation.

G.8.25. Georgiev G., Argirov Y., Mechkarova T., Stoyanova A., Fractographic Research on Samples after Fatigue Testing in the Destruction Zone, International Journal "NDT Days", Volume III, Issue 2, Year 2020, eISSN: 2603-4646, pp. 110-114

Purpose: The article presents a methodology for fractographic studies of samples after fatigue tests in the failure zone. For the purposes of this research, experimental samples of duplex steel were made SAF2507 (ASTM S32750).

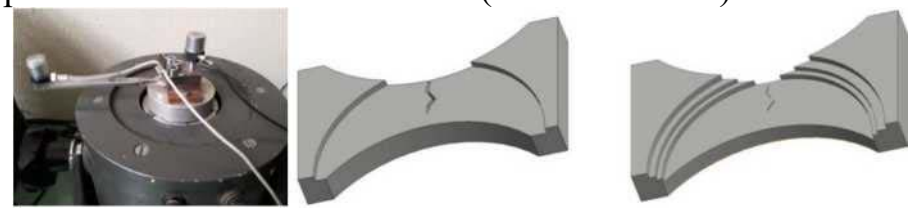

Fig. 47. Installation with a vibromass for the study of fatigue and mirroring the methodology for fractographic studies with layer-by-layer removal of material

Fig. 48. At least two points are measured with an indicator clock

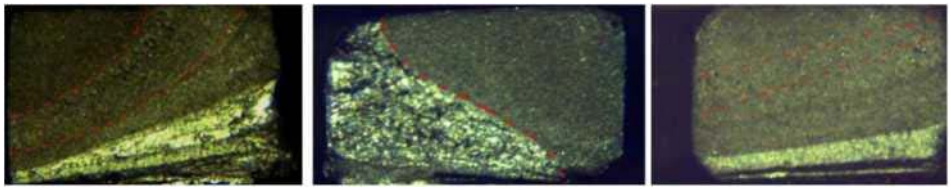

Fig. 49. Macrostructures of profiles at the crack development front

The methodology used to trace the crack in depth, is a fractographic methodology, with the help of which it is possible to clearly determine the type, direction and size of the fatigue crack at different depth. Upon reaching the selected length and depth of the crack, the specimen is measured for flatness in the area of the crack. An indicator clock attached to the magnetic stand is used, allowing extremely accurate measurement of deviations in the surfaces.

Conclusion: After the conducted experiments it is localized the location and the moment of origin of the tired focus is established crack of the experimental specimens subjected to multicycle fatigue.

G.8.26. Spasova D., Argirov Y., Mechkarova T., Investigation of The Strength and Elastic Characteristics of Elastic Rope Used in Safety Equipment, International Journal "NDT Days", Volume III, Issue 5, Year 2020, eISSN: 2603-4646, pp . 307-312

Purpose: The work contains results of experimental research in laboratory conditions of the strength and elastic characteristics of elastic rope used in rescue equipment

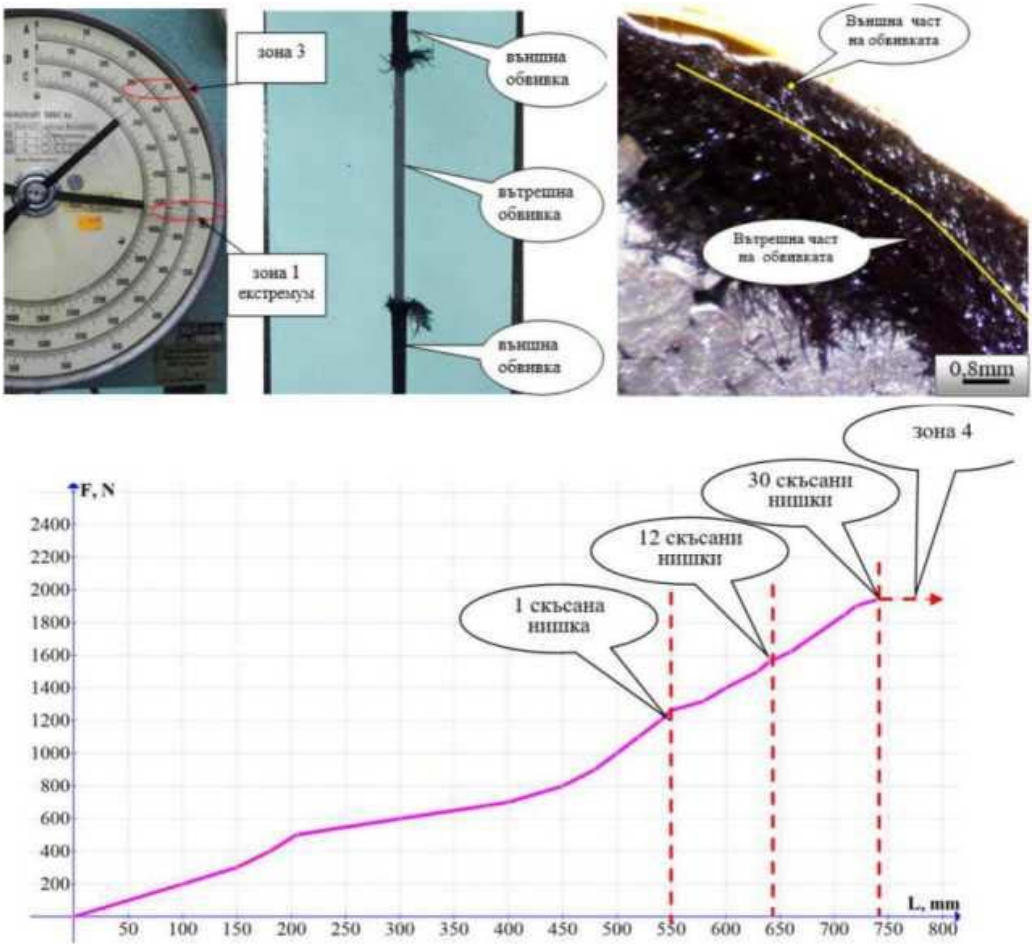

Fig. 50. Tensile test results

The subject elastic rope is made of a rubber core and double outer shell of high-quality polyamide fabric, with high strength and elastic characteristics. The inner part of the outer shell has higher mechanical characteristics (withstands up to a load of 2850 N and relative elongation A = 1738%), as opposed to external A = 867%), which shows that the use of this kind of elastic rope has a double protection, which in turn enables timely intervention at case of an accident.

Conclusion: From the research done it was found that the research object - an elastic rope, a product of the German company JUMBO-Textil is suitable for use on rescue equipment in the shipping industry.

G.8.27. Mechkarova T., Argirov Y., Spasova D., Stoyanova A., Structural Changes of Nitrogen Ferrite After Aging in Temperature Interval up to 100 °y, The annals of "Dunarea de Jos" University of Galati fascicle IX. metallurgy and materials science, No. 1 - 2021, ISSN 2668-4748; e-ISSN 2668-4756, DOI: https://doi.org/10.35219/mms.2021.1.04, pp.28-33

Objective: This paper aims to determine the extent of aging of nitrogen ferrite at temperatures below 100 °C and the structural and strength changes that occur in the process. The tests are carried out on samples of technically pure iron (Armco). The specimens are pre-deformed by tension and re-crystallisation heating to achieve a large-grain ferrite structure. A large-grained structure has been chosen to more accurately track the change in micro-hardness of the individual grains during the aging process. Nitric ferrite results from gas carbonitriding and subsequent hardening. Upon hardening, the samples are stored in a refrigerator, and then the surface layer formed is removed through electrochemical corrosion. Afterwards, aging heat treatment at temperatures below 100 °C is undertaken. After the aging process, micro-hardness of the individual grains is examined and X-ray structural analysis is performed.

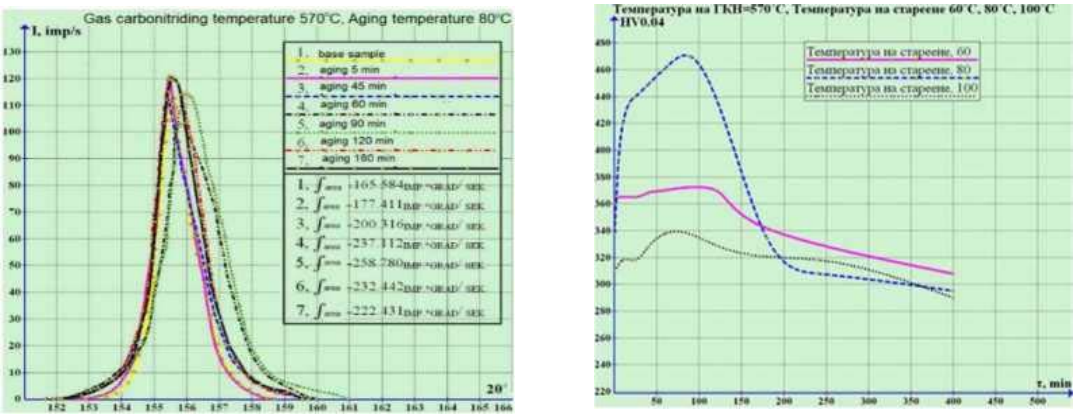

Fig. 51. X-ray phase and microstructural analyses

Conclusion: In conclusion, it should be noted that the saturated nitrogen ferrite formed has a tendency to age after low temperature gas carbonitriding, its strength indicating the greater increase in a temperature range of 80-90 °C (470 HV) when retained at these temperatures from 40 to 70 minutes. For aging processes, these optimal temperature ranges and aging time turn out to be too narrow, due to the high sensitivity of the coherent interaction between the nitride phase (α") and the ferrite matrix (α).

G.8.28. Petrova D., Argirov Y., Mechkarova T., Investigation of the Aging Process of Bronze Alloys from Thracian Time Found in the Area of Byala, Bulgaria, International Journal "NDT Days", Volume IV, Issue 2, Year 2021, eISSN: 2603-4646, pp. 135-138

Purpose: The article investigates the aging process of bronze alloys from Thracian time, found in the region of Byala, Bulgaria. The investigated copper coins, are of the 40 Numia type of Emperor Justinian I (AD 527-565), minted in the city of Nicomedia, Byzantium.

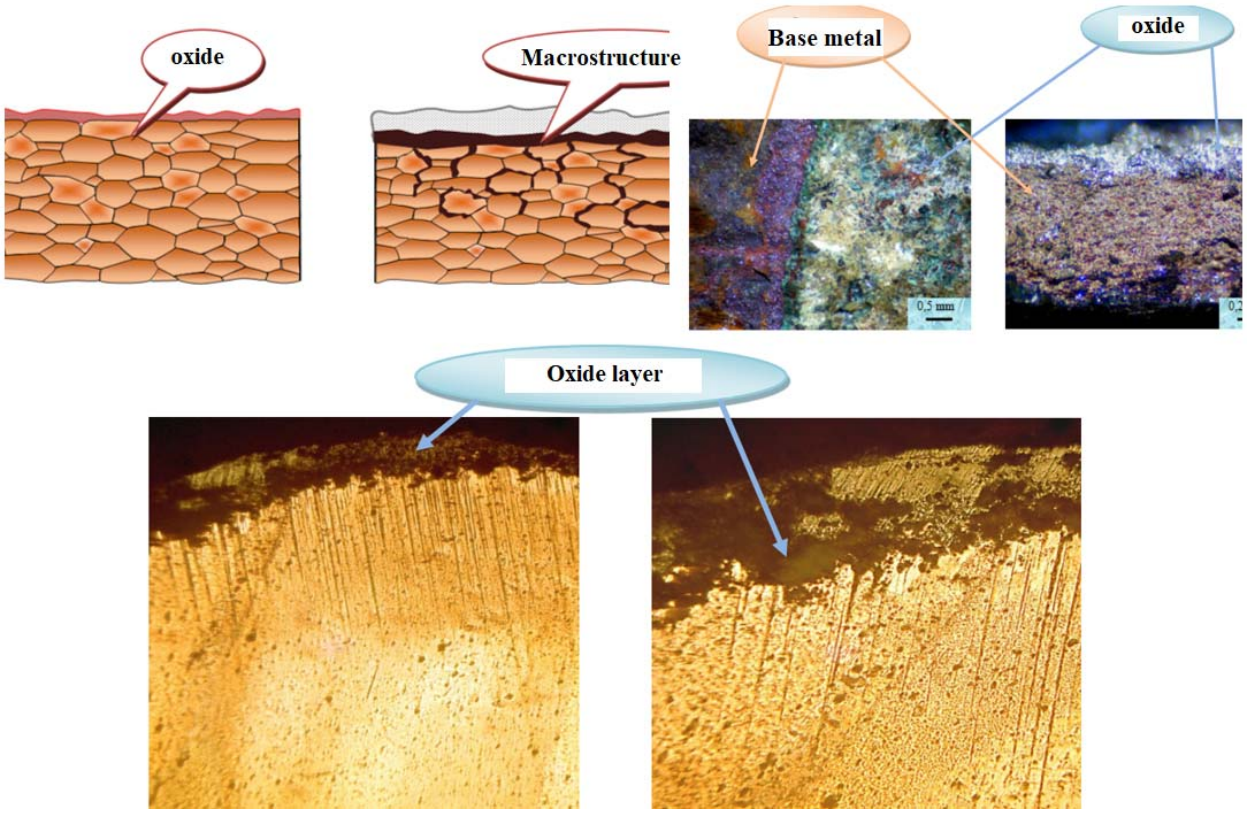

Fig. 52. Macro and microstructures of the studied objects magnitute X125

Conclusion:

After thousands of years of oxidation, the patina has formed a thick layer around the metal, and the oxides are not only on the surface, but they have also penetrated around the grains, in the core of the metal. This affects the the mechanical characteristics of the metal, making it brittle and brittle.

G.8.29. Mechkarova T., Argirov Y., Atanasov N., Spasova D., Technology and Equipment for Annealing on a Welded Strip from GS-50CrV4, International Journal "NDT Days", Volume IV, Issue 4, Year 2021, eISSN: 2603-4646, pp. 238-242

Purpose: This paper analyzes technology and equipment for heat treatment of welded rail made of GS-50CrV4 steel.

Fig. 53. General view of the welded joint of the GS-50CrV4 (SEW 835) steel rail and the measured Vickers hardnesses HV5.

Fig. 54. Flame quenching and subsequent low-temperature quenching retort at 200oC

Fig. 55. Results of surface hardness measurements

Conclusion: The obtained results for the macrohardnesses are indicative that the manufactured technology for repair restoration of spring steel GS-50CrV4 (SEW 835) in the shop is suitable.

D.8.30. Nikolova R., Petrov P., Mechkarova T., Investigation Welded Joints of Steel 110G13L, International Journal "NDT Days", Volume IV, Issue 2, Year 2021, eISSN: 2603-4646, pp. 128-134

Objective: The present article investigates repair recovery through welding of steel 110G113L.

Stages of technology for their repair restoration:

1. Preliminary mechanical treatment for cleaning
2. Welding: Current source "KRACRA" G500, ROW welding with thick-coated basic electrode EN 65y11y3
3. Cleaning: Actually, the top layer of metal was removed from the working surface.
4. Heat treatment to remove residual stresses: heating to about 320-350°C and slow and uniform cooling for 1 hour in the furnace.

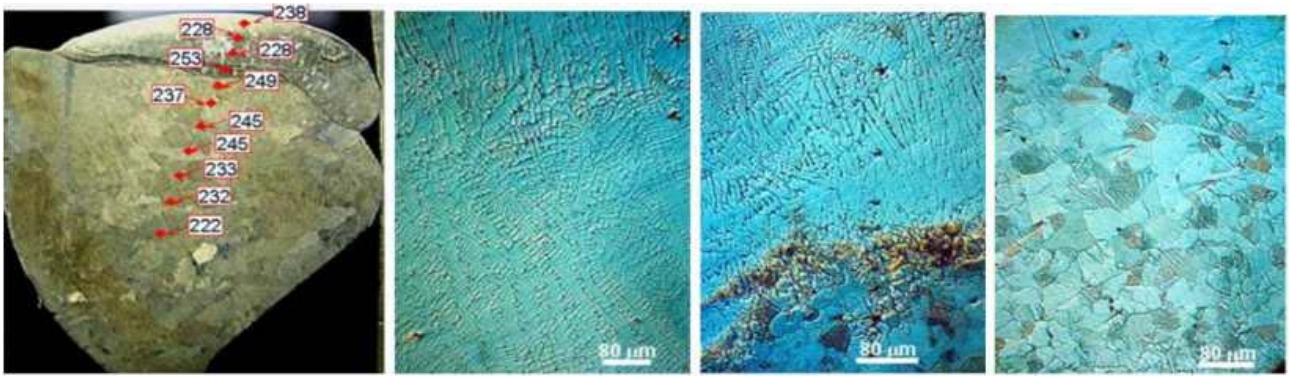

Fig. 56. Macrostructure with measured Vickers microhardnesses and microstructures in weld metal, fusion zone and base metal

Conclusion:

The metallographic analysis of steel samples 110G13 at REDZ showed that no macrodefects such as cracks, pores, non-metallic inclusions, undercuts, etc., and in the microstructural analysis, the base metal structure is an austenitic phase with a dendritic character.

Hardnesses are in the range of 254-283. Hardnesses change relatively uniform in depth to the base metal. Highest hardness values are noticeable in the heat affected zone (HTZ) in the welded metal and the overheating zone - on both sides of the boundary of alloying.

G.8.31. Mechkarova T., Antonov G., Nikolov D., Determination of Residual Resource and Reliability of Vertical Tanks for Petroleum Products, International Journal "NDT Days", Volume V, Issue 2, Year 2022, eISSN: 2603-4646, pp. 90-97

Purpose: The publication deals with determining the residual resource of utilization and reliability of steel vertical storage tanks of petroleum products.

When surveying the site, the following non-destructive tests were carried out tests:

1. Summary report of a general visual inspection of the bottom, roof, hull, as well as the foundation of the tank.

2. Ultrasonic hull thickness measurement. The assessment of the residual resource of the tank is carried out accord current standard RD 26-10-87.

Selection of minimum number of measurements

δ	γ	N при υ_h						
		0,1	0,2	0,3	0,4	0,6	0,8	1,0
0,10	0,80	-	5	10	13	32	50	100
	0,90	3	8	15	32	65	125	200
	0,95	5	13	25	50	100	200	400
	0,99	8	25	50	100	200	400	650

Mantel т. №	Working weight, mm	Measured weight, mm	depth of destruction, mm
1	9,0	7,8	1.2
2	9,0	7,9	1.1
3	9,0	7,5	1.5

Conclusion:

The obtained results for the thicknesses by non-destructive testing and the presented methodology allows to make a statistical assessment of reliability indicators (average and specified service life, average and specified failure-free operation time), from which to establish the remaining operational resource of the tank. With a bigger one non-uniformity of corrosion destruction from the selected may destruction of the investigated elements of the object occurs before it occurs its limit state.

The minimum thicknesses measured are sufficient to accommodate the the hydrostatic loads in tank operation provided that the geometry of the tank does not contradict the requirements of the standard EN14015, and the maximum fill level is 15.8m and the volumetric weight of the stored product does not exceed 1.01/m3.

G.8.32. Nikolova R., Petrov P., Mechkarova T., MMA Welding of the Rotary Shredder for Household Waste from S690Q Steel, ISSN: 2603-4018, International Journal "NDT Days", Volume V, Issue 3, Year 2022, eISSN: 2603 -4646, pp.140-145

Purpose: The article is about welding the teeth of a device for shredding household waste from steel S690Q. The repair of the teeth of the rotary crusher starts by separating the defective elements from the rotor of the machine. This is followed by electric arc welding in a protective gas chamber environment (MIG method) and shielding gas argon on the crusher rotor beds. Welding the worn teeth of the crusher with coated electrodes UTP DUR 600, with a diameter of the electrode wire 03.2x350. These are basic electrodes UTP, with a hardness of 60HRC, for hard alloy welding of workpieces subjected to combined impact loading and abrasive wear (BDS EN ISO 14700: E Fe8, DIN 8555: E 6-UM-60)

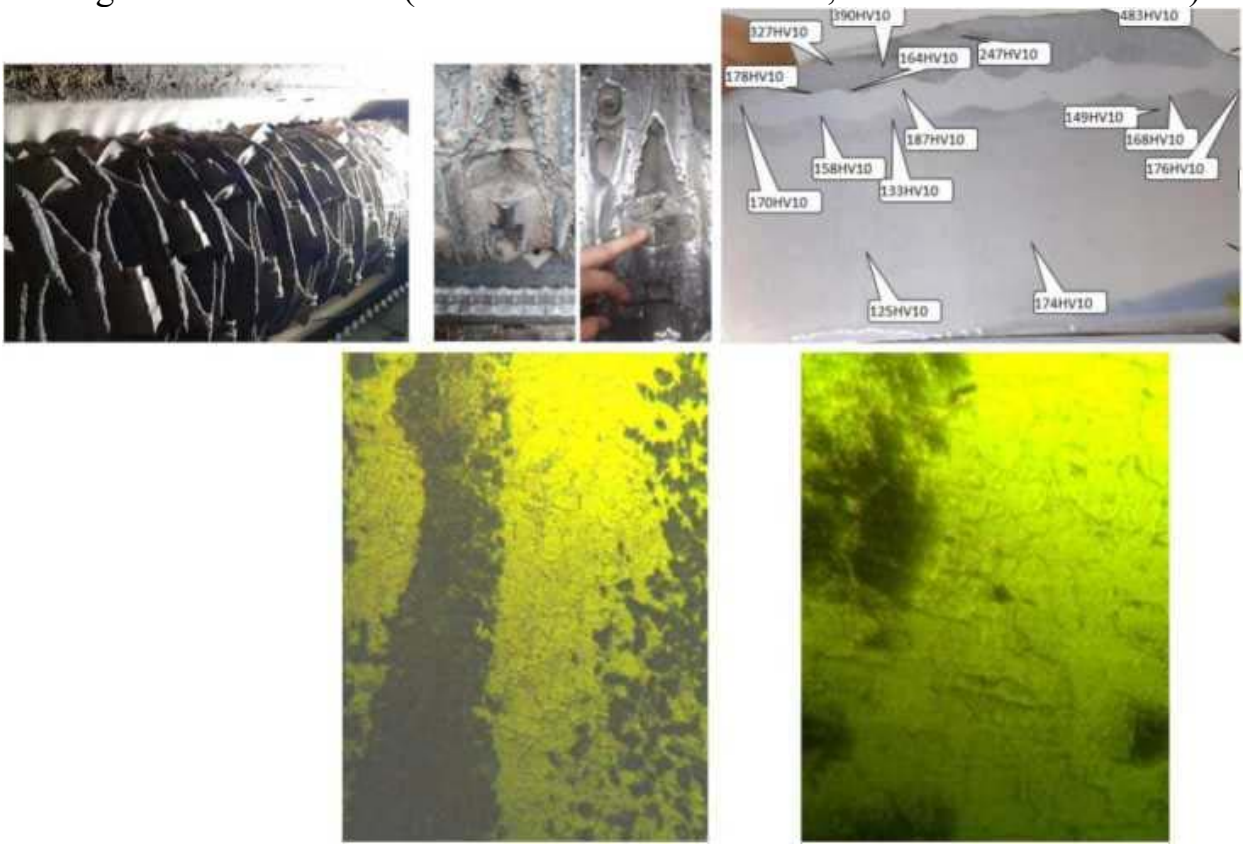

Fig. 57. Macrostructure, measured Vickers microhardnesses and microstructures of the fusion zone and the base metal

Conclusion: The microstructural analysis of the welded layers showed that the base material of S690Q steel is in different structural a condition possibly due to differences in rolling technology of the steel and varying degrees of texturing. The measured hardness in of the welded layers is significantly higher than that of the base material steel, which implies increased surface wear resistance of the products.

G.8.33. Serhiy Ryabchenko, Yaroslav Argyrov, Tetiana Mechkarova, GRINDING OF FUEL MATERIALS WITH SPECIAL ALLOY DIAMOND ABRASIVE HEADS, Issue 26. INSTRUMENTAL MATERIALS SCIENCE, UDC 621.923 DOI: 10.33839/2708-731y-24-1-369-375, p 369-375, ISSN 2708-731X, Institute approved materials im. V.M. Bakulya

Purpose: Study of wear efficiency with different composition abrasive tools. The effectiveness of surface treatment with special alloys is an urgent problem in the manufacture and repair of equipment. The biggest problem in handling landfilled materials is delivery quality and physical-mechanical condition of the processed surface. They were conducted wear tests with various abrasive tools on welded layer on a special duplex alloy (SAF 2507) and was evaluation of processing efficiency (material removal and abrasive wear). For surface treatment are used abrasive heads with a diameter of 10 mm from white and chrome electrocorundum, silicon carbide and synthetic diamond.

Fig. 58. Used heads for grinding high-speed tool chrome electrocorundum, silicon carbide, white corundum, artificial diamond, welded duplex steel plate.

Conclusion:

The abrasive heads made of chromium corundum and synthetic diamond provide the highest wear efficiency. They have a high percentage of withdrawal of the surface material (up to 0.25 mm/min) and minimal wear of the abrasive layer.

D.8.34. Mechkarova T., Argirov Ya., Ryabchenko S.V. , Making of methodology for quality control of structure and properties of stainless steel products from the food industry, XVIII International conference «Strategy of quality in industry and education» 05-08 June 2023, Varna, Bulgaria M A T E R I A L I XVIII International Conference «Strategy of Quality in Industry and Education» June 5 - June 8, 2023, Varna, Bulgaria

Purpose: The report deals with the development of a methodology for quality control of structure and properties of stainless steel products SS304 used in the food industry. Results of corrosion wear - *solution - 3% sea salt in H2O*

Time of detention	**Output**	**40h**	**80h**	**120h**	**144h**
Sample no	**Mass in grams after corrosion wear T=60y, solution - 3% sea salt in H2O**				
1	**0.590**	**0.586 0.58**		**0.585**	**0.585**
2	**1.231**	**1.230**	**1.230**	**1.229**	**1.229**
3	**1.187**	**1.187**	**1.186**	**1.186**	**1.186**
4	**1,090**	**1,090**	**1,090**	**1,090**	**1,090**

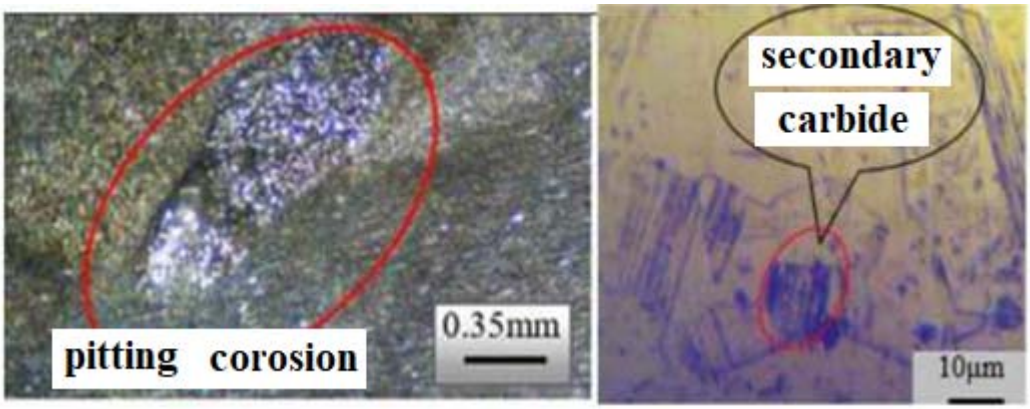

Fig. 59. Microstructures

Conclusion: From the conducted corrosion wear, it turns out that with the weakest corrosion protection is sample 3. This sample is the bottom of a deeply drawn object from the food industry. At the macroanalysis showed pitting corrosion, and after 80 hours corrosive effects are observed and pitting corrosion. After the established 80 hours passivation of the defected areas is observed the site and cessation of corrosion development. Of the conducted microstructural studies, a coarse-grained structure with grain sizes above 50ym and secondary carbide separations. The availability of carbides and their inhomogeneous distribution, leads to local formation of corrosion.

D.8.35. Tatyana Mechkarova, Nikolay Valchev, Genesis of Destruction Steel Flange of Auto Concrete Pump, Bulgarian Society for NDT International Journal "NDT Days", Volume IV, Issue 2, ISSN: 2603-4018, eISSN: 2603-4646, https://www .bg-s-ndt.org/journal/vol6/JNDTD-v6-n2- a08.pdf

Purpose: The object of study is a steel assembly that performs rotary movement called the "fifth wheel" of a concrete pump. Due of continuous work about 10 years of operation and unexercised regular technical inspection of the boom of the concrete pump (no regulatory requirements for this) a crack has formed which causes failure of the technical facility. This requires research and analysis of the causes that led to the formation and development of the crack.

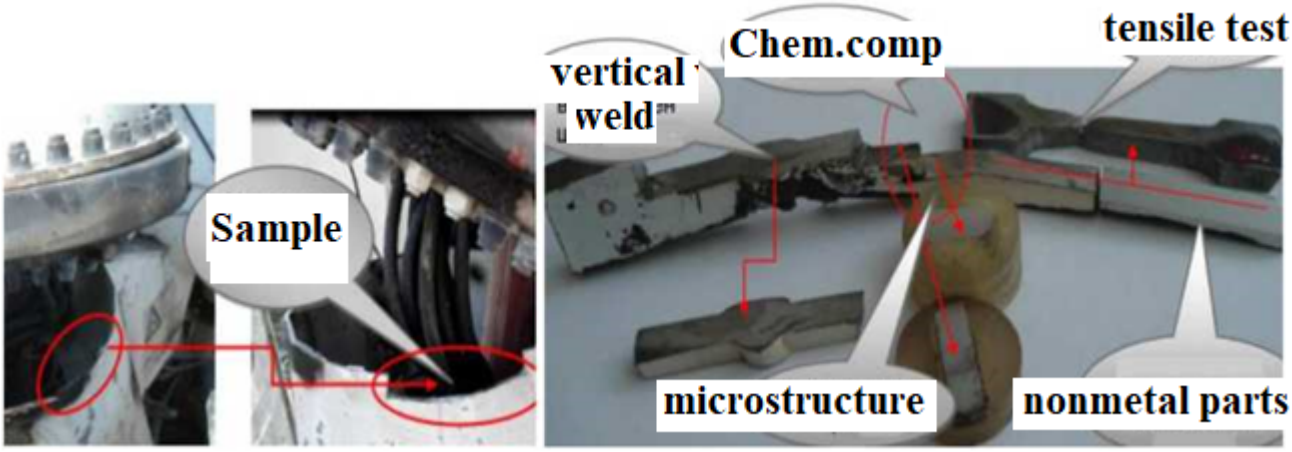

Fig. 60. Object of research

Conclusion: Regarding the chemical composition of the steel from the witness, the exact chemical composition was established and the brand of was determined the steel used is S700MC (1.8974) EN 10149-2-1996. It's steel applicable in heavily loaded constructions and has good weld ability.

Regarding the second part of the study, the presence of non-metallic inclusions. The texture of the metal is defined, which is a sign for cold rolled steel. Texture has an effect on mechanical properties, therefore tensile testing failed yield strength (ReH), and conditional strength (R0.2). This caused an increase in strength properties, but it can adversely affect the fatigue strength, especially in the bending zone. The observation of microcracks in the scrap during strength (tensile) testing is a sign of non-density of the metal due to a number of factors (non-metallic inclusions, especially linear, linear grouping of pearlite colonies, additional tilting in the bending zone).

D.8.36. Nikolay Valchev, Tatyana Mechkarova, Nikolay Nikolov, Investigation of Cylindrical and Flatten Specimens with Thin Diffusion Layers, Volume IV, Issue 3, ISSN: 2603-4018, eISSN: 2603-4646, https:// www.bg-s-ndt. org/journal/vol6/JNDTD-v6-n3-a07.pdf

Objective: In the present work, methods for the study of thin diffusion layers with metallographic methods. The studies are carried out with flat, cylindrical or complex profile test bodies with thin diffusion layers applied to their surfaces. In these samples the preparation of the microslides is more special due to the small thickness of the layer about 10μm. This makes the connection between the clamp and the sample difficult, so as it is necessary to ensure full contact, for receiving after the grinding of a sharp edge between the perpendicular planes of micro grind, not round. This enables precise focusing at high magnifications in the area of study a thin diffusion layer.

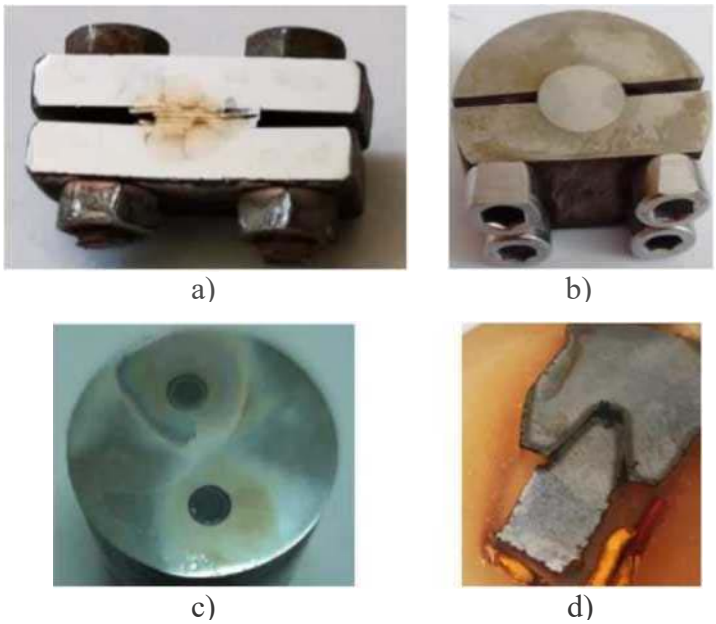

Fig. 61. Microsections of samples with different geometry shape and thin diffusion layers: a-flat specimens; b- cylindrical samples; c- small bushings; d- gears

Conclusion: The presented methodology for the study of thin diffusion layers of samples of different shapes and sizes f applicable to strengthening methods (nitriding, carbonitriding) where requires studying the thickness of the diffusion layer, its structure and microhardness in depth.

D.8.37. Nikolay Nikolov, Tatyana Mechkarova, Nikolay Valchev, Methodology of Hybrid Welding Layering and Cladding on Flat Surfaces, Bulgarian Society for NDT International Journal "NDT Days", Volume IV, Issue 1, ISSN: 2603-4018, eISSN: 2603-4646, https ://www.bg-s-ndt.org/ journal/vol6/JNDTD-v6-n3-a07.pdf Purpose:

In the present work, a variety of methods for formation of protective layers by combining the classic methods of plasma powder coating with semi-automatic methods filler wire welding (MAG).

The need to combine classical methods arises from creating protective layers of expensive and rare metals and alloys laid down on widely used base metals with relatively low cost. The possibilities for the application of the hybrid methods is as for obtaining layers on the surfaces of newly built metal structures, as well as for repair restoration processes for existing defective ones, where replacing the equipment with a new one is economically unprofitable.

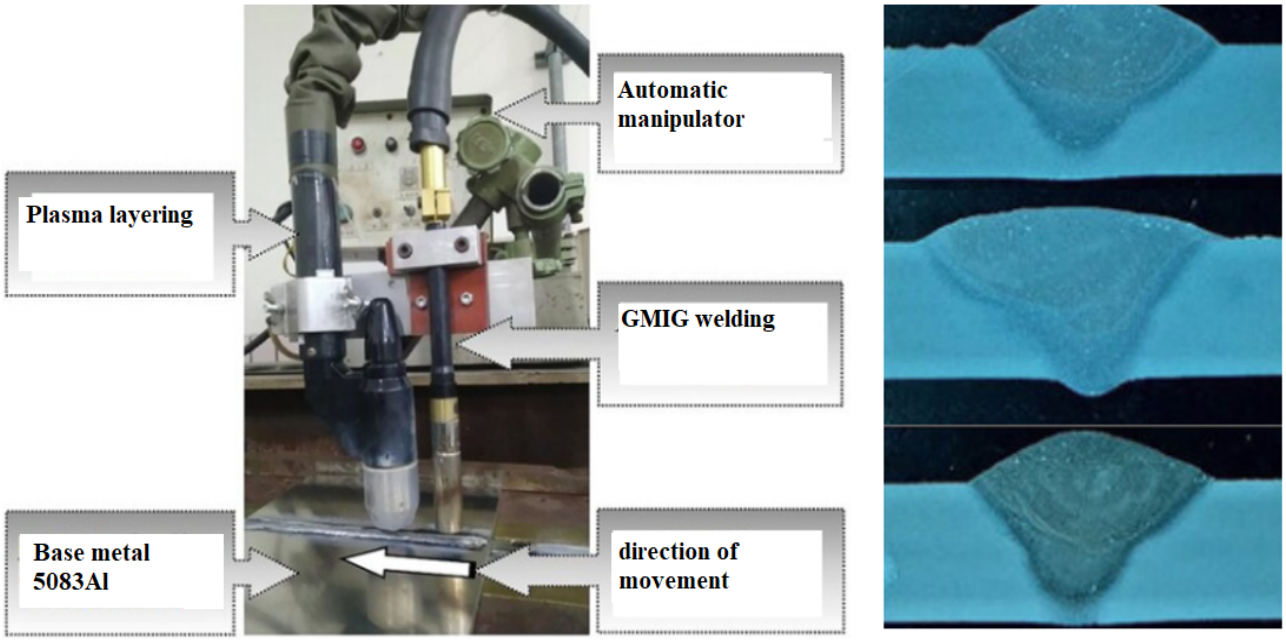

Fig. 62. Combined Plasma-MIG layering

Conclusion: Combined methods are gaining popularity mainly in repair and restoration technologies, where the replacement of a defective one technological equipment is many times more expensive than its restoration. The technologies for hybrid or combined use of the classical methods of [illegible] application and when making new equipment when their [illegible] rare.

Заличена информация по Регламент (ЕС) 2016/679

Дата: 29.02.2024 г.

Подпис:
/ас. д-р инж. Татяна Мечкарова /